

1 **Transcriptional profiles predict treatment outcome in**
2 **patients with tuberculosis and diabetes at diagnosis and at**
3 **two weeks after initiation of anti-tuberculosis treatment**

4 **Authors**

5 Cassandra L.R. van Doorn^{1,#}, Clare Eckold^{2,#}, Katharina Ronacher^{3,4}, Rovina Ruslami^{5,6},
6 Suzanne van Veen¹, Ji-Sook Lee², Vinod Kumar^{7,8}, Sarah Kerry-Barnard⁹, Stephanus T.
7 Malherbe³, Léanie Kleynhans³, Kim Stanley³, Philip C. Hill¹⁰, Simone A. Joosten¹, Reinout
8 van Crevel^{8,11}, Cisca Wijmenga⁷, Julia A. Critchley⁹, Gerhard Walzl³, Bacht Alisjahbana^{5,6},
9 Mariëlle C. Haks¹, Hazel M. Dockrell², Tom H. M. Ottenhoff¹, Eleonora Vianello^{1*} and
10 Jacqueline M. Cliff^{2*}, on behalf of the TANDEM Consortium[§]

11 [#]These authors contributed equally to this work

12 ^{*}These authors contributed equally to this work

13

14 **Correspondence:**

15 Dr. Eleonora Vianello

16 Email: e.vianello@lumc.nl

17 Telephone: +31 71 52 63844

18 ORCID: 0000-0003-0342-4055

19

NOTE: This preprint reports new research that has not been certified by peer review and should not be used to guide clinical practice.

20 ¹Department of Infectious Diseases, Leiden University Medical Center, Leiden, The
21 Netherlands

22 ²Dept of Infection Biology and TB Centre, London School of Hygiene & Tropical Medicine,
23 London, WC1E 7HT, United Kingdom

24 ³SA MRC Centre for TB Research, DST/NRF Centre of Excellence for Biomedical
25 Tuberculosis Research, Division of Molecular Biology and Human Genetics, Faculty of
26 Medicine and Health Sciences, Department of Biomedical Sciences, Stellenbosch University,
27 Cape Town, South Africa

28 ⁴Mater Research Institute – The University of Queensland, Translational Research Institute,
29 Brisbane, QLD, Australia

30 ⁵TB-HIV Research Center, Faculty of Medicine, Universitas Padjadjaran, Bandung, Indonesia

31 ⁶Hasan Sadikin General Hospital, Bandung, Indonesia

32 ⁷University of Groningen, University Medical Center Groningen, Department of Genetics,
33 Groningen, the Netherlands

34 ⁸Department of Internal Medicine and Radboud Center for Infectious Diseases, Radboud
35 University Medical Center, Nijmegen, the Netherlands

36 ⁹Population Health Research Institute, St George's Hospital Medical School, University of
37 London.

38 ¹⁰Centre for International Health, Division of Health Sciences, University of Otago, Dunedin,
39 New Zealand

40 ¹¹Centre for Tropical Medicine and Global Health, Nuffield Department of Medicine,
41 University of Oxford, Oxford, UK

42

43 **Abstract**

44 **Background**

45 Globally, the anti-tuberculosis (TB) treatment success rate is approximately 85%, with
46 treatment failure, relapse and death occurring in a significant proportion of pulmonary TB
47 patients. Treatment success is lower among people with diabetes mellitus (DM). Predicting
48 treatment failure early after diagnosis would allow early treatment adaptation and may improve
49 global TB control.

50 **Methods**

51 Samples were collected in a longitudinal cohort study of adult TB patients with or without
52 concomitant DM from South Africa and Indonesia to characterize whole blood transcriptional
53 profiles before and during anti-TB treatment, using unbiased RNA-Seq and targeted gene
54 dcRT-MLPA.

55 **Findings**

56 We report differences in whole blood transcriptome profiles, which were observed before
57 initiation of treatment and throughout treatment, between patients with a good versus poor anti-
58 TB treatment outcome. An eight-gene and a 22-gene blood transcriptional signature
59 distinguished patients with a good treatment outcome from patients with a poor treatment
60 outcome at diagnosis (AUC=0.815) or two weeks (AUC=0.834) after initiation of anti-TB
61 treatment, respectively. High accuracy was obtained by cross-validating this signature in an
62 external cohort (AUC=0.749).

63 **Interpretation**

64 These findings suggest that transcriptional profiles can be used as a prognostic biomarker for
65 treatment failure and success, even in patients with concomitant DM.

66 **Funding**

67 The research leading to these results, as part of the TANDEM Consortium, received funding
68 from the European Community's Seventh Framework Programme (FP7/2007-2013 Grant
69 Agreement No. 305279) and the Netherlands Organization for Scientific Research (NWO-TOP
70 Grant Agreement No. 91214038).

71

72 **Keywords (4-6)**

73 Biomarkers, tuberculosis, treatment outcome, diabetes mellitus

74

75 Introduction

76 With more than 10 million new cases and approximately 1.5 million deaths annually,
77 tuberculosis (TB), which is caused by *Mycobacterium tuberculosis* (*Mtb*), continues to be a
78 major global health threat.¹ Upon infection with *Mtb*, 5-10% of adults develop active disease
79 during their lifetime and one quarter of the world's population is estimated to be latently
80 infected with *Mtb* (LTBI). The global anti-TB treatment success rate is only about 85% and
81 even lower in patients with multi-drug resistant TB or with comorbidities like HIV or diabetes
82 mellitus (DM)¹⁻³, resulting in a significant number of patients with poor clinical outcomes.

83 DM triples the risk of developing active TB⁴ and increases the risk of poor clearance of
84 the infection following anti-TB treatment.⁵⁻⁷ In 2020, 0.37 million TB cases were estimated to
85 suffer from DM comorbidity.¹ 85-95% of all DM cases is attributed to type-2 diabetes mellitus
86 (T2DM).⁸ Since global DM prevalence is estimated to rise from 463 million people in 2019 to
87 700 million in 2045⁹, in particular in areas where TB is endemic, there is increasing concern
88 about the consequences of the rising DM prevalence for global TB control.¹ The mechanisms
89 underlying DM-induced treatment failure remain, however, poorly understood.

90 Prediction of treatment failure based on sputum-smear microscopy and mycobacterial
91 culture lacks sensitivity¹⁰ and depends on the quality of sputum samples, which are difficult to
92 collect and are frequently inconsistent in quality.¹¹⁻¹³ In addition to more advanced sputum-
93 based diagnostics, monitoring of whole blood transcriptomics may be an additional,
94 complementary but independent method to monitor treatment responses, possibly with
95 increased sensitivity.¹⁴ Numerous studies have reported transcriptional biomarker profiles for
96 active TB and response to anti-TB treatment using whole-blood or PBMCs in settings with
97 varying TB incidence.¹⁵⁻²⁰ In addition, multiple studies have demonstrated the predictive
98 potential of host gene biomarkers in identifying patients at risk of developing active TB, relapse
99 and treatment failure.²¹⁻²⁸ Together, these studies showed that gene signatures may have utility

100 at predicting anti-TB treatment success versus failure already early after TB diagnosis,
101 providing a significant improvement over the currently used low sensitivity conversion to
102 negative sputum-based culture testing.¹⁰ Despite the high incidence of DM and pre-DM among
103 TB patients in TB-endemic settings^{7,29-31}, only a few studies have identified or validated such
104 signatures in TB patients with DM or hyperglycemia.^{32,33}

105 Characterizing transcriptomic profiles may improve our understanding towards the
106 immunological pathways that are involved in DM-associated TB pathology and monitoring
107 treatment success and failure in TB patients with concomitant DM is key to combat the
108 tuberculosis-diabetes (TB-DM) co-epidemic. Although the blood transcriptome profile of TB-
109 DM patients is more similar to TB patients than to DM patients, suggesting a dominant
110 influence of active TB infection, we and others recently demonstrated significant differences
111 in the blood transcriptome of TB-DM patients compared to TB patients.^{32,33} Additionally, the
112 transcriptomic profiles of patients with TB-related intermediate hyperglycemia (TBrel-IH)
113 were similar to the profiles of TB-DM patients.³² Importantly, we also showed that DM
114 comorbidity lowered the performance of published diagnostic biomarker signatures.³²
115 Therefore, there is a need for biomarkers that predict treatment success and failure in TB
116 patients independently of their glycemia or DM status.

117 The aim of the current study was to identify blood transcriptional gene signature for
118 predicting the anti-TB treatment outcome at an early stage after initiation of anti-TB treatment,
119 irrespective of concomitant DM. We combined an unbiased RNA-Seq approach and a selective
120 dcRT-MLPA approach (a multiplex RT-PCR platform) as two independent strategies to
121 identify gene signatures with high discriminatory power to distinguish patients with a good
122 treatment outcome from patients with a poor treatment outcome. Host gene biomarker profiles
123 to identify anti-TB treatment success or failure could facilitate the evaluation of new anti-TB

124 drugs and improve clinical surveillance of TB patients, even in settings with high DM
125 incidence.

126

127 **Methods**

128 *Study participant recruitment, classification and treatment*

129 Adult pulmonary TB patients were recruited as part of the TANDEM project²⁹ in two locations:
130 Bandung in Indonesia (UNPAD) and Cape Town in South Africa (SUN). All TB patients were
131 newly diagnosed and microbiologically confirmed, and included people with TB-DM. The TB-
132 DM group included participants with both pre-diagnosed DM and newly identified DM, with
133 new diagnosis based on a laboratory HbA1c test $\geq 6.5\%$ with a confirmatory HbA1c test $\geq 6.5\%$
134 or fasting blood glucose ≥ 7 mmol/L at TB diagnosis²⁹, followed by a further HbA1c test $\geq 6.5\%$
135 after 6 months of TB treatment. The TB patients without DM included people with a normal
136 glycaemic index (laboratory HbA1c $< 5.7\%$) at TB diagnosis (“TB-only”). Patients whose
137 HbA1c test results were $\geq 5.7\%$ and $< 6.5\%$ at both TB diagnosis and at 6 months were deemed
138 to have pre-diabetes (“TB-preDM”) and patients with raised glycaemia at TB diagnosis but
139 below the cut-off for DM diagnosis ($5.7\% \leq$ laboratory HbA1c $< 6.5\%$) were deemed to have
140 TB-related intermediate hyperglycaemia (“TBrel-IH”). In South Africa, healthy controls
141 without TB or DM were also recruited for baseline sample analysis. Multi-drug-resistant TB,
142 HIV positivity, pregnancy, serious co-morbidity and corticosteroid use were exclusion criteria.
143 TB patients received standard first line TB treatment according to WHO Guidelines.
144 Microbiological measures recorded at baseline and throughout treatment included sputum
145 smear and culture, with time to positivity (TTP) in mycobacteria growth indicator tubes
146 (MGIT) also assayed in South Africa. TB patients were classified based on their treatment
147 outcome: “poor treatment outcome” included those patients who died, failed initial treatment
148 (remained sputum positive at five months) or experienced TB-recurrence in the 12 month

149 follow-up period post treatment, whilst those with “good treatment outcome” had successful
150 TB treatment without subsequent recurrence. Patients for whom the outcome data were missing
151 were not included in downstream analyses. Most TB-DM patients received local standard of
152 care DM treatment, whilst a subgroup in Indonesia received more intensive HbA1c monitoring
153 and treatment adjustment through TB treatment as part of a pragmatic randomised control
154 trial.³⁴

155 Ethics Statement

156 The study was approved by the London School of Hygiene & Tropical Medicine Observational
157 Research Ethics Committee (6449), the SUN Health Research Ethics Committee (N13/05/064)
158 and the UNPAD Health Research Ethics Committee, Faculty of Medicine, Universitas
159 Padjadjaran (number 377/UN6.C2.1.2/ KEPK/ PN), and participants gave written informed
160 consent.

161 RNA sample collection and extraction

162 Patient samples were collected prior to initiation of treatment (diagnosis), at weeks 2, 4, 8, 16
163 and 26 through treatment, and at 12 months after TB diagnosis, and from HC at baseline only.
164 Venous blood (2.5ml) was collected into PAXgene Blood RNA Tubes (PreAnalytiX). Total
165 RNA was extracted using RNeasy spin columns (Qiagen) and quantified by Nanodrop
166 (Agilent). The LabChip GX HiSens RNA system (PerkinElmer) was used for quality
167 assessment of samples processed by RNA-Seq.

168 Unbiased RNA-Seq of global gene expression

169 Samples collected at TB diagnosis and weeks 2, months 2, and months 6 from the first 63
170 participants recruited were analysed by RNA-Seq (Table 1). Libraries were generated using the
171 poly-A tail Bioscientific NEXTflex-Rapid-Directional mRNA-Seq method with the Caliper
172 SciClone. Single-end sequencing was performed using the NextSeq500 High Output kit V2

173 (Illumina) for 75 cycles. Sequence data from FASTQ files were aligned to the Human g1kv37
174 reference genome, using STAR (v2.5.1b).³⁵ Quality control was performed with FastQC³⁶,
175 while transcript quantification was performed using HT-seq count (v0.61)³⁷: lowly expressed
176 transcripts (<50 counts across all samples), were removed from the downstream analysis.
177 RNA-Seq data were normalised using DESeq2 (v1.30.0).³⁸

178 Dual-color Reverse-Transcriptase Multiplex Ligation-dependent Probe Amplification (dcRT-
179 MLPA)

180 Dual-color reverse-Transcriptase Multiplex Ligation-dependent Probe Amplification (dcRT-
181 MLPA) was performed on all samples to identify blood transcriptional profiles as described
182 previously.³⁹ Brief descriptions are provided in the Supplementary Information. RT primers
183 and half-probes were designed by Leiden University Medical Centre (LUMC, Leiden, The
184 Netherlands) and encompassed sequences for 144 selected key immune-related genes to profile
185 the innate, adaptive and inflammatory immune responses (Supplementary Table S1), and four
186 housekeeping genes (*GAPDH*, *ABR*, *GUSB*, *B2M*). Genes with an adjusted p-value <0.05
187 (Benjamini-Hochberg⁴⁰) and a log₂-fold change (FC) <-0.6 and >0.6 were considered
188 differentially expressed genes (DEGs). Genes that were below the detection limit in >90% of
189 the samples per cohort were excluded from analysis.

190 Data analysis and Statistics

191 Statistical analyses to compare participant demographics were carried out using GraphPad
192 Prism 8 software (Graphpad Software, San Diego, CA, USA). For continuous measures, a
193 Mann-Whitney U-test was used when comparing two groups and a Kruskal-Wallis test when
194 comparing three groups. For non-continuous measures, the Chi-square test was used. P-values
195 as <0.05 were considered significant.

196 Molecular Degree of Perturbation (MDP) analysis was performed by R using *mdp* R
197 package⁴¹, and differences between the mean ranks of the groups were assessed by Mann-
198 Whitney U test followed by Benjamini-Hochberg False discovery correction.⁴⁰ Cell population
199 estimates were calculated using the *cellCODE*⁴² R package, with the *IRIS*⁴³ and *DMAP*⁴⁴ data
200 sets used as a reference. Modular analysis was performed using the R package *tmod*⁴⁵ and
201 its *HGtest* method, with DEGs used as the foreground and all genes used as the background
202 signal.

203 Differential expression analysis (DEA) was performed in R using the *MaSigPro*
204 package⁴⁶ to characterise longitudinal differential gene expression of genes measured by RNA-
205 Seq: this followed a two-step regression method, finding genes with significant temporal
206 expression changes and also significant differences between clinical groups. A quadratic
207 regression model was executed due to the number of timepoints analysed. The regression
208 model treats time as a quantitative variable so differentially expressed are not only detected,
209 but also changes in trends and magnitude.

210 Longitudinal DEA of genes measured by dcRT-MLPA was assessed by means of linear
211 mixed models for repeated measures over time using *lme4* package in R.⁴⁷ A Benjamini-
212 Hochberg False discovery correction was performed, with an adjusted p-value of <0.05 deemed
213 significant. Non-parametric Mann-Whitney U-test followed by Benjamini-Hochberg
214 correction was performed to identify DEGs between patients who had a good and poor
215 treatment outcome. Correlations were evaluated using Pearson's correlation coefficient.

216 Treatment outcome signatures based on dcRT-MLPA data were identified in TB
217 patients of South Africa and Indonesia using Recursive Feature Elimination (RFE)⁴⁸ and
218 Random Forest (RF). Because the number of patients with a good treatment outcome was
219 considerably larger than those with a poor treatment outcome (poor, n=38; good, n=134), a
220 random down-sampling technique as well as a Synthetic Minority Oversampling Technique

221 (SMOTE) were applied to balance the classes (i.e. “good treatment outcome” and “poor
222 treatment outcome”) of the dataset.⁴⁹ RF was performed as machine learning algorithm on the
223 dataset including the selected genes and the performance of gene signatures was evaluated by
224 Leave-One-Out Cross Validation (LOOCV).^{50,51} We assessed the classifying performance of
225 the model by evaluating Receiver Operating Characteristic (ROC) curve and Area Under the
226 ROC Curve (AUC) with 95% Confidence Interval (CI). An extended description of the data-
227 analysis methods is provided in the Supplementary Information.

228

229 Role of Funders

230 Funders had no role in study design, data collection, data analyses, data interpretation, writing
231 of the report and decision to submit the paper for publication.

232

233 **Results**

234 Study Design and Cohort

235 Pulmonary TB patients were recruited into the prospective longitudinal study in South Africa
236 and Indonesia, and followed up through standard treatment and for the following 12 months.
237 Altogether, 39 TB patients of the 176 recruited had a “poor treatment outcome”, with 7
238 patients dying, 26 failing treatment (based on continued sputum smear or culture positivity at
239 month 6), and 6 experiencing recurrences in the subsequent 18 months. The “poor treatment
240 outcome” rates were similar in the two sites (Table 1). The median age of the patients was
241 equal in patients with either a good or poor treatment outcome (median = 47 years), with a
242 higher proportion of males with a poor treatment outcome than a good treatment outcome (56%
243 and 67% respectively). The proportion of TB patients with DM with a poor treatment outcome
244 (15/39; 38%) was slightly higher than that with a good treatment outcome (44/137; 32%),

245 whereas the proportion with TBrel-IH was higher in those with a good treatment outcome
246 (65/137; 47%) than a poor treatment outcome (14/39; 36%). There was no evidence that those
247 who had a poor treatment outcome had more severe TB at diagnosis, with similar sputum
248 bacterial loads (as measured by TTP) in TB patients from South Africa and similar sputum
249 smear grade in Indonesia across the good and poor treatment outcome groups.

250 Poor treatment outcome was reflected by an attenuated treatment response compared to good
251 treatment outcome

252 The holistic unbiased analysis of gene expression in TB patients with good or poor treatment
253 outcomes by RNA-Seq approach was performed on a subset of study participants (Table 1).
254 There were significant changes in global gene expression in patients with a good treatment
255 outcome continuously through TB treatment, reflecting treatment response (Figure 1A). Gene
256 expression perturbation was also evident in patients who had a poor treatment outcome,
257 although the sample score was higher at diagnosis compared to patients who had a good
258 treatment outcome. This represents differences at the transcriptomic level between patients
259 with a good versus a poor treatment outcome, already before initiation of anti-TB treatment.
260 This was followed by less change over time in response to TB treatment in the poor TB
261 outcome group.

262 Next, we focused our molecular distance analysis on 144 TB-associated genes as
263 measured by dcRT-MLPA, which was performed on all study participants (n=201) (Table 1).
264 Again, there were significant changes in global gene expression continuously through TB
265 treatment in patients with a good treatment outcome, but not in patients with a poor treatment
266 outcome (Figure 1B), reflecting an attenuated TB treatment response. Despite the substantial
267 treatment response in patients who had a good treatment outcome, gene expression perturbation
268 did not completely normalize to levels of healthy controls by 6 months (Supplementary Figure
269 S1).

270 Together, these data suggest that there was a different biosignature in those with good
271 versus poor treatment outcomes, which was reflected by transcriptomic differences before
272 initiation of anti-TB treatment and by a tempered response to anti-TB treatment in patients with
273 a poor treatment outcome compared to patients with a good treatment outcome.

274 *Global Differential expression in patients who had good or poor responses to TB treatment*

275 The changes in gene expression in the RNA-Seq data through time and between the patients
276 with a good or poor treatment outcome were analyzed by MaSigPro, initially in the South
277 African and Indonesian cohorts separately. The strength in this method was that it was able to
278 monitor the change in dynamics over time and also between different treatment groups. In
279 South Africa, the genes which changed differently through time between the patients with good
280 or poor treatment outcome were grouped into nine clusters (Supplementary Figure S2A,
281 Supplementary Table S2), with an increase in expression through treatment in four clusters
282 (1,2,3,5), a decrease in four clusters (4,6,7,8), and no change in one cluster (9). Genes with
283 higher expression throughout treatment in TB patients with poor treatment outcome were
284 grouped in seven clusters (1,3,4,5,7,8,9) and those with higher expression in TB patients with
285 a good treatment outcome were grouped in two clusters (2,6). A similar pattern was observed
286 in the Indonesian cohort, with DEGs identified through treatment between good and poor
287 separating into nine clusters (genes increasing in clusters 2,5,7, and decreasing in clusters
288 1,3,4,6,8,9) (Supplementary Figure S2B, Supplementary Table S3), with higher expression in
289 either the good or poor treatment outcome group. Importantly, these differences in gene
290 expression through time were observed in all TB patient groups, irrespective of their DM status.

291 The genes grouped into the clusters in the Indonesian and South African cohorts
292 partially overlapped but there was variability. A third MaSigPro analysis was therefore
293 conducted, to find those genes which were differentially expressed through treatment between
294 TB patients with a good or poor treatment outcome, irrespective of their geographical origin

295 (Figure 2, Supplementary Table S4). Again, the genes differentially expressed through
296 treatment in the combined analysis separated into nine clusters, with variable patterns of
297 expression over time and between TB patients with good or poor treatment outcome. Some
298 clusters (2,5,6) contained genes which were different between the groups at all time points,
299 whereas other clusters (1,3,4,5,7,8,9) were similar at some timepoints and more divergent at
300 others (Figure 2, Table 2).

301 The number of transcripts within each cluster in the combined analysis ranged from 4
302 to 47 (Table 2), with the majority of genes identified in all clusters encoding proteins. There
303 were also various regulatory transcripts in some clusters, including long non-coding RNAs,
304 miRNA, snoRNA, retained introns, as well as antisense, nonsense-mediated decay,
305 overlapping senses and sense intronic transcripts. To understand the biological function of the
306 DEGs, the transcripts within each cluster were analysed using the g:COST tool within the
307 g:Profiler application⁵², to determine significant enrichment of genes in Gene Ontology (GO)
308 molecular function, cellular component and biological process categories, as well as in curated
309 biological pathways from KEGG and Reactome databases and the CORUM protein database.
310 Genes in cluster 2 were largely involved in B cell receptor signalling, seen in the GO and
311 pathway analyses, and these were more highly expressed in people who had a poor treatment
312 outcome, with increasing expression through treatment. This upregulation of genes involved in
313 B cell function, particularly those involved in earlier stages of B cell development, was not
314 related to the overall number of B cells in the samples, as predicted from the samples using
315 CellCode analysis package (Supplementary Figure S3). Cluster 9 was predominantly
316 composed of immunoglobulin transcripts, whose expression decreased much more
317 substantially in patients with a good treatment outcome. The largest gene cluster (4) was
318 enriched with genes involved in actin remodelling, including the Arp 2/3 complex, and in
319 pathways related to infections with bacteria such as *Shigella*, *E. coli*, *Yersinia* and *Salmonella*.

320 Cluster 7 contained genes related to mitotic cell division, and these were more highly expressed
321 in patients with a poor treatment outcome (Table 2). These analyses were also performed using
322 the DAVID online tool⁵³, and similar results were obtained (not shown). The DEGs found in
323 the combined and separate cohort MaSigPro analyses were used as a foreground against all
324 genes in a modular analysis using the Tmod package, which gives biological function to a gene
325 list. It showed an upregulation of genes involved in B cell function in good versus poor
326 treatment outcomes, in both the Indonesian and South African cohorts (Supplementary
327 Table S5).

328 *Identification of DEGs through TB treatment in patients with good or poor treatment*
329 *outcomes*

330 Next, we focused our DEA on 144 genes that previously have been associated with TB³⁹ using
331 dcRT-MLPA (Supplementary Table S6). No significant DEGs were detected by directly
332 comparing patients with a good versus a poor treatment outcome at the indicated timepoints
333 (Supplementary Figure S4), and therefore we analyzed longitudinal expression of genes.
334 Kinetic profiling of DEGs identified 16 DEGs in patients with a good treatment outcome and
335 12 DEGs in patients with a poor treatment outcome. The longitudinal expression of DEGs
336 identified by dcRT-MLPA showed a significant correlation with genes measured by RNA-Seq,
337 highlighting the validity and reproducibility of our approach (Supplementary Figure S5). A
338 high correlation between DEGs of patients who had a poor treatment outcome and DEGs of
339 patients who had a good treatment outcome could be detected ($R=0.87$, $p<0.0001$),
340 highlighting the challenge of discriminating patients with a good versus a poor treatment
341 outcome based on single genes (Supplementary Figure S6). Genes associated with active
342 TB^{15,20,54} or risk of developing TB²² were substantially downregulated (*GBP1*, *GBP2*, *GBP5*,
343 and *IFITM3*) or upregulated (*GPLY* and *PRF1*) over time in TB patients regardless of their
344 treatment outcome, reflecting transcriptomic response to anti-TB treatment (Figure 3A and

345 Supplementary Figure S7). Other genes associated with active TB were significantly down- or
346 upregulated (*STAT2*, *MMP9*, *IRF7*, *IFI6*, *IFIT2*, *IFIT3*, and *CCR7*) during anti-TB treatment
347 in patients who had a good treatment outcome, but not in patients who had a poor treatment
348 outcome, or vice versa (*CD3E*, *PTPRCV1*, *NLRP1*, *BCL2*)^{15,39,54,55}. The expression of *TAGAP*,
349 previously associated with active TB⁵⁵, was significantly increased during anti-TB treatment
350 in patients who had a poor treatment outcome. Modular analysis showed that the gene profile
351 of regulated genes was dominated by genes in the interferon (IFN) signaling pathway,
352 especially in patients who had a good treatment outcome (Figure 3B).

353 Identification of a signature predicting treatment outcome

354 Machine learning algorithms were implemented on data obtained at each time point to develop
355 biomarker panels to predict treatment outcomes at different stages of TB treatment. First, we
356 aimed to identify gene signatures from RNA-Seq analysis on a subset of subjects, but we found
357 a low performance of gene signatures generated on diagnosis, week two and month six
358 (AUC=0.625, AUC=0.667 and AUC=0.615, respectively) to predict treatment outcome,
359 potentially due to a low number of patients in the training and test set (Supplementary Figure
360 S8A). The best performing model was built on month two resulting in an AUC of 0.8667
361 (Supplementary Figure S8A, Supplementary Table S7). We also tested an active TB disease
362 biomarker signature, namely the three-gene Sweeney signature²⁰, to determine whether it
363 resolved significantly more in those with a good treatment outcome than in those with a poor
364 treatment outcome. This signature has previously been shown to persist in patients with
365 persistent lung inflammation²⁶. However, in our RNA-Seq data, this signature revealed an AUC
366 of 0.5333 (Supplementary Figure S8B) highlighting that the process behind poor treatment
367 outcome cannot be predicted by expression of these three genes.

368 Next, we aimed to identify early correlates of treatment outcome by implementing
369 machine learning algorithms on gene expression as measured by dcRT-MLPA. We focused

370 our analysis on the identification of gene predictors at diagnosis and at week two that could
371 possibly be used in future studies to predict the occurrence of poor or good treatment outcome
372 before or early after anti-TB treatment initiation, first by down-sampling the good treatment
373 outcome class. The top eight ranked genes (*GBP1*, *FCGR1A*, *STAT1*, *IFITM3*, *BCL2*, *CCLA*,
374 *TLR9*, *CD274*) from the diagnosis signature were used for RF machine learning model
375 implementation (Table 3). Excitingly, the signature had a high predictive power (AUC=0.815)
376 to classify TB patients with a good or poor treatment outcome, already before anti-TB treatment
377 initiation (Figure 4A). Furthermore, the gene signature showed high performance on the
378 cohorts separately (South Africa, AUC=0.845; Indonesia, AUC=0.744). Next, we investigated
379 whether accuracy could be improved by predicting treatment outcome after initiation of anti-
380 TB treatment, thus measuring the early treatment response. We identified a 22-gene signature
381 to predict treatment outcome at two weeks after initiation of anti-TB treatment (Table 3). The
382 performance of the week two signature in predicting treatment outcome was slightly improved
383 (AUC=0.834) compared to the diagnosis signature, especially in patients from the Indonesian
384 cohort (AUC=0.867 versus AUC=0.744 at diagnosis). Furthermore, we identified a 14-gene
385 month two signature, which, however, demonstrated a slightly lower accuracy in predicting
386 treatment outcome compared to diagnosis and week two gene signatures (AUC=0.791).

387 Since we detected differences in the kinetics of gene expression of patients who had a
388 good treatment outcome versus patients with a poor treatment outcome (Figure 1), we next
389 assessed whether a “delta” gene signature, by subtracting week two values from diagnosis,
390 could improve the predictive performance. The delta signature encompassed seven genes
391 (*GNLY*, *MRC1*, *GBP5*, *NLRP1*, *FLCN1*, *ZNF532*, and *IFIT2*) and slightly improved predictive
392 performance (pooled cohorts, AUC=0.849; South Africa, AUC=0.839 and Indonesia,
393 AUC=0.872) compared to the week two and diagnosis signatures (Supplementary Figure S9,
394 Supplementary Table S8). Multiple genes were included in more than one gene signature

395 (Supplementary Figure S10A), of which four genes (*GBP1*, *GBP5*, *FCGR1A*, *INDO*) are
396 shown in Figure 4B. Next, we validated performance of the diagnosis signature and month two
397 signature on an independent validation cohort²⁸, which like our cohorts, included diabetic
398 patients. Our diagnosis gene signature had high predictive power on the Indian validation
399 cohort (AUC=0.749) (Figure 4C). The week two and delta signatures could not be validated
400 on the Indian cohort, because samples were not collected two weeks after initiation of anti-TB
401 treatment in this cohort. Three genes (*CD3E*, *PTPRCv1*, *NOD2*) that were included in our gene
402 signatures, were also part of gene signatures described by Sivakumaran et al. (Supplementary
403 Figure S10B). Finally, we assessed whether gene signatures with improved performance could
404 be obtained by applying SMOTE⁴⁹ as an alternative sampling technique. A diagnosis SMOTE
405 gene signature was obtained that showed overlap with the diagnosis gene signatures obtained
406 by random down-sampling (Supplementary Table S9, Supplementary Figure S10C). The
407 SMOTE signature produced a high degree of accuracy in discriminating patients with a good
408 treatment outcome from patients with a poor treatment outcome, but performed with lower
409 accuracy compared to the diagnosis signature obtained by random down-sampling (pooled
410 cohorts, AUC=0.728; South Africa, AUC=0.695; Indonesia, AUC=0.765) (Supplementary
411 Figure S11). The diagnosis SMOTE signature exerted a similar predictive capacity on the
412 external Indian cohort compared to the down-sampling signature (SMOTE, AUC=0.704;
413 down-sampling, AUC=0.749).

414 Taken together, we identified gene signatures with high predictive power on treatment
415 outcome, irrespective of DM as comorbidity, in patients from South Africa and Indonesia and
416 in patients from the external Indian validation cohort.

417

418 Discussion

419 In this study, we identified peripheral blood transcriptional signatures which predict anti-TB
420 treatment success and failure in TB patients with or without concomitant hyperglycaemia or
421 DM. Previous studies developing biomarker signatures of TB treatment success, recurrence or
422 failure^{24-26,56} did not include people with DM comorbidity, and we have previously found
423 concomitant DM impairs existing TB diagnosis signature accuracy.³² Here we showed DM
424 also affects existing TB treatment-response biomarker signatures in the RNA-Seq dataset,
425 suggesting that they should be derived with cohorts including this population.

426 Our whole cohort dataset, from which we generated treatment outcome signatures, was
427 derived using our dcRT-MLPA gene set, which did not contain most of the genes reported in
428 previous signatures, except *GBP5*, which was included in our week two and month two gene
429 signatures. Sivakumaran et al.²⁸ recently reported baseline and month two gene signatures
430 predicting treatment outcome at six months after initiation of anti-TB treatment, using the same
431 material (whole blood), technique (dcRT-MLPA) and gene set. Notably, our treatment outcome
432 gene signatures showed some overlap with the signatures reported by Sivakumaran et al.
433 (*CD3E*, *PTPRCv1*, *NOD2*), suggesting that these genes are useful in predicting treatment
434 outcome independently of ethnical background. Furthermore, our treatment outcome gene
435 signatures showed overlap of genes of the TB risk signature predicting TB progression from
436 healthy controls more than a year before onset of TB (*GBP1*, *GBP2*, *GBP5*, *FCGR1A*, *STAT1*,
437 *TAP1*).²² Within our study, 12 genes (*BCL2*, *BMP6*, *CCL13*, *CD209*, *FCGR1A*, *GBP1*, *GBP5*,
438 *INDO*, *MMP9*, *MRC1*, *STAT1*, *TLR9*) were overlapping between gene signatures, including
439 both the gene signatures obtained by down-sampling and the gene signatures obtained by
440 SMOTE. The occurrence of genes in multiple gene signatures within this study and between
441 studies highlights the power of transcriptomic biomarkers in predicting treatment outcome and

442 suggests that universal biomarkers can be applied to cohorts of different ethnicity and
443 independently of the DM/glycaemia status of TB patients.

444 Patients with a poor treatment outcome responded to anti-TB treatment at the level of
445 individual genes, as detected by downregulation of genes (*GBP1, GBP2, GBP5, IFITM3*) that
446 have been associated with active TB and upregulation of genes (*CD3E, PTPRCv1, NLRP1,*
447 *GNLY, PRF1, BCL2*) that show lower expression in patients with active TB compared to LTBI
448 or healthy controls^{15,20,39,55}. However, MDP analysis showed that the response to anti-TB
449 treatment was diminished in those with a poor treatment outcome compared to patients who
450 had a good treatment outcome. Notably, the majority of genes that were significantly
451 downregulated in patients who had a good treatment outcome, but not in patients who had a
452 poor treatment outcome, are involved in IFN signaling (*IRF7, IFIT2, IFIT3, STAT2, IFI6,*
453 *TAP2*). This suggests that a poor treatment outcome was reflected by persisting IFN signaling
454 response and supports a role for type I IFN signaling in TB pathogenesis.^{15,57}

455 *TAGAP* was significantly increased in patients who had a poor treatment outcome in
456 the pooled South African and Indonesian cohort as well as in both cohorts separately. *TAGAP*
457 encodes T-cell activation Rho-GTPase-activating protein, however, the exact role of *TAGAP*
458 in *Mtb* pathogenesis is currently unknown. Several studies have linked *TAGAP* with active TB;
459 *TAGAP* was enriched for differential acetylation peaks upon *Mtb* infection in granulocytes⁵⁸
460 and *TAGAP* was induced upon vaccination with AERAS-402 vaccine encoding a fusion protein
461 of *Mtb* antigens.⁵⁹ Furthermore, *TAGAP* had higher expression in TB patients compared to
462 LTBI and healthy controls⁵⁵ and, surprisingly, lower expression in pulmonary TB compared to
463 household controls.⁶⁰ Our data showing that *TAGAP* expression was significantly increased
464 during anti-TB treatment in patients who had a poor treatment outcome could indicate that
465 *TAGAP* is actively involved in TB pathogenesis or that *TAGAP* expression is a consequence of
466 persisting *Mtb* infection, but this remains to be investigated.

467 There are several limitations of the current study. First, the sample size in this study
468 was not based on an a priori power calculation, as this study was part of a larger study
469 investigating differences in gene expression in patients with varying degrees of hyperglycemia.
470 To increase statistical power, we therefore pooled patients from two cohorts (South Africa and
471 Indonesia), which introduced heterogeneity within the studied groups. However, this can also
472 be a strength, potentially increasing application over different ethnic backgrounds. Second,
473 there were missing values in the cohort study. The missing values occurred as a result of
474 random drop-outs or technical errors caused by low quantity or quality of some samples, and
475 therefore the use of linear mixed models for the DEA most likely produced unbiased results.
476 Third, although the prevalence of hyperglycaemia/DM is not indicated in the majority of other
477 TB biomarker studies, which is a limitation of these studies considering the rising incidence of
478 TB-DM comorbidity, our study contained many patients with high HbA_{1c} levels. Although
479 this may have introduced a bias, the strength of this approach is that treatment outcome
480 signatures have been developed that can be applied to patients independently of their
481 glycaemia/DM status. Furthermore, we showed that our eight-gene diagnosis signature had a
482 high performance (AUC=0.749) when tested on an external validation cohort in patients with
483 a different ethnic background (India), which is striking since geographic or ethnic variations
484 may significantly impact on the immune responses to TB.

485 In this study, we demonstrated the potential of gene signatures to predict treatment
486 outcome, in a cohort including patients with concomitant DM or hyperglycaemia. Identification
487 of a diagnosis gene signature containing only eight genes in this study, and even fewer genes
488 in signatures reported by others^{26,27}, indicates that clinically-implementable biomarker
489 signatures can be developed using transcriptomic-based approaches using easily accessible
490 whole blood, and that are promising as surrogate marker for sputum culture conversion.

491

492 **Contributors**

493 Study concept and design: BA, RvC, RR, PCH, GW, SAJ, JAC, MCH, HMD, THMO, JMC;
494 Patient recruitment, Sample collection, processing and selection: BA, KR, STM, LK, PCH,
495 KS, RR, GW; Clinical database design, curation, maintenance: SK-B, JAC;
496 Laboratory Experiments and data acquisition: CE, SvV, JSL, JMC; Data Analysis and
497 interpretation: CLRvD, CE, SvV, VK, SAJ, CW, MCH, HMD, THMO, EV, JMC; Writing the
498 manuscript: CLRvD, CE, SAJ, HMD, THMO, EV, JMC; Critical Revision of the manuscript:
499 CLRvD, CE, KR, STM, SAJ, PCH, JAC, MCH, HMD, THMO, EV, JMC; All authors read
500 and approved the final version of the manuscript.

501 **Declaration of Interests**

502 GW had patents to methods of tuberculosis diagnosis and to tuberculosis biomarkers unrelated
503 to the current study. The rest of the authors declare no financial or commercial conflicts of
504 interest.

505 **Acknowledgements**

506 The authors acknowledge all participants involved in this study. The authors
507 acknowledge Bahram Sanjabi, Desiree Brandenburg-Weening, and Pieter van der Vlies for
508 assistance with the RNA-Seq, Evelien Temminck for providing technical assistance
509 with dcRT-MLPA experiments, Erni Durdevic for providing statistical and machine
510 learning advice, and Prof. Dr. Harleen Grewal and Dr. Dhanasekaran Sivakumaran for
511 providing datafiles of the cross-validation dataset.

512 **Data Sharing Statement**

513 RNA sequence data have been submitted to NCBI Gene Expression Omnibus (GEO) under
514 accession number GSE193979. dcRT-MLPA data can be found in Supplementary Table S6.

515 References

- 516 1. World Health Organization. Global tuberculosis report 2021. Geneva: World Health
517 Organization. Licence: CC BY-NC-SA 3.0 IGO., 2021.
- 518 2. Alemu MA, Yesuf A, Girma F, et al. Impact of HIV-AIDS on tuberculosis treatment outcome
519 in Southern Ethiopia–A retrospective cohort study. *Journal of Clinical Tuberculosis and Other*
520 *Mycobacterial Diseases* 2021; **25**: 100279.
- 521 3. Huangfu P, Ugarte-Gil C, Golub J, Pearson F, Critchley J. The effects of diabetes on
522 tuberculosis treatment outcomes: an updated systematic review and meta-analysis. *Int J Tuberc Lung*
523 *Dis* 2019; **23**(7): 783-96.
- 524 4. Jeon CY, Murray MB. Diabetes mellitus increases the risk of active tuberculosis: a systematic
525 review of 13 observational studies. *PLoS med* 2008; **5**(7): e152.
- 526 5. Baker MA, Harries AD, Jeon CY, et al. The impact of diabetes on tuberculosis treatment
527 outcomes: a systematic review. *BMC medicine* 2011; **9**(1): 1-15.
- 528 6. Dooley KE, Tang T, Golub JE, Dorman SE, Cronin W. Impact of diabetes mellitus on
529 treatment outcomes of patients with active tuberculosis. *The American journal of tropical medicine*
530 *hygiene* 2009; **80**(4): 634.
- 531 7. Alisjahbana B, Sahiratmadja E, Nelwan EJ, et al. The effect of type 2 diabetes mellitus on the
532 presentation and treatment response of pulmonary tuberculosis. *Clinical Infectious Diseases* 2007;
533 **45**(4): 428-35.
- 534 8. Tuomilehto J. The emerging global epidemic of type 1 diabetes. *Current diabetes reports*
535 2013; **13**(6): 795-804.
- 536 9. Saeedi P, Petersohn I, Salpea P, et al. Global and regional diabetes prevalence estimates for
537 2019 and projections for 2030 and 2045: Results from the International Diabetes Federation Diabetes
538 Atlas. *Diabetes research and clinical practice* 2019; **157**: 107843.
- 539 10. Horne DJ, Royce SE, Gooze L, et al. Sputum monitoring during tuberculosis treatment for
540 predicting outcome: systematic review and meta-analysis. *The Lancet infectious diseases* 2010; **10**(6):
541 387-94.
- 542 11. Bhat J, Rao V, Muniyandi M, Yadav R, Karforma C, Luke C. Impact of sputum quality and
543 quantity on smear and culture positivity: findings from a tuberculosis prevalence study in central
544 India. *Transactions of the Royal Society of Tropical Medicine Hygiene* 2014; **108**(1): 55-6.
- 545 12. Hernández P, Punchak M, Camacho M, Hepple P, McNerney R. Investigating the quality of
546 expectorated sputum for tuberculosis diagnosis in Bolivia. *The International Journal of Tuberculosis*
547 *and Lung Disease* 2015; **19**(9): 1065-7.
- 548 13. Meyer AJ, Atuheire C, Worodria W, et al. Sputum quality and diagnostic performance of
549 GeneXpert MTB/RIF among smear-negative adults with presumed tuberculosis in Uganda. *PLoS One*
550 2017; **12**(7): e0180572.
- 551 14. Warsinske H, Vashisht R, Khatri P. Host-response-based gene signatures for tuberculosis
552 diagnosis: A systematic comparison of 16 signatures. *PLoS medicine* 2019; **16**(4): e1002786.
- 553 15. Berry MP, Graham CM, McNab FW, et al. An interferon-inducible neutrophil-driven blood
554 transcriptional signature in human tuberculosis. *Nature* 2010; **466**(7309): 973-7.
- 555 16. Bloom CI, Graham CM, Berry MP, et al. Detectable changes in the blood transcriptome are
556 present after two weeks of antituberculosis therapy. *PloS one* 2012; **7**(10): e46191.
- 557 17. Cliff JM, Lee JS, Constantinou N, et al. Distinct phases of blood gene expression pattern
558 through tuberculosis treatment reflect modulation of the humoral immune response. *J Infect Dis* 2013;
559 **207**(1): 18-29.
- 560 18. Kaforou M, Wright VJ, Oni T, et al. Detection of tuberculosis in HIV-infected and-uninfected
561 African adults using whole blood RNA expression signatures: a case-control study. *PLoS Med* 2013;
562 **10**(10): e1001538.
- 563 19. Maertzdorf J, McEwen G, Weiner 3rd J, et al. Concise gene signature for point-of-care
564 classification of tuberculosis. *EMBO molecular medicine* 2016; **8**(2): 86-95.
- 565 20. Sweeney TE, Braviak L, Tato CM, Khatri P. Genome-wide expression for diagnosis of
566 pulmonary tuberculosis: a multicohort analysis. *The Lancet Respiratory Medicine* 2016; **4**(3): 213-24.

- 567 21. Scriba TJ, Penn-Nicholson A, Shankar S, et al. Sequential inflammatory processes define
568 human progression from M. tuberculosis infection to tuberculosis disease. *PLoS Pathog* 2017; **13**(11):
569 e1006687.
- 570 22. Zak DE, Penn-Nicholson A, Scriba TJ, et al. A blood RNA signature for tuberculosis disease
571 risk: a prospective cohort study. *The Lancet* 2016; **387**(10035): 2312-22.
- 572 23. Mistry R, Cliff JM, Clayton CL, et al. Gene-expression patterns in whole blood identify
573 subjects at risk for recurrent tuberculosis. *J Infect Dis* 2007; **195**(3): 357-65.
- 574 24. Cliff JM, Cho J-E, Lee J-S, et al. Excessive cytolytic responses predict tuberculosis relapse
575 after apparently successful treatment. *The Journal of infectious diseases* 2016; **213**(3): 485-95.
- 576 25. Thompson EG, Du Y, Malherbe ST, et al. Host blood RNA signatures predict the outcome of
577 tuberculosis treatment. *Tuberculosis* 2017; **107**: 48-58.
- 578 26. Warsinske HC, Rao AM, Moreira FM, et al. Assessment of validity of a blood-based 3-gene
579 signature score for progression and diagnosis of tuberculosis, disease severity, and treatment response.
580 *JAMA network ope* 2018; **1**(6): e183779-e.
- 581 27. Suliman S, Thompson EG, Sutherland J, et al. Four-gene pan-African blood signature predicts
582 progression to tuberculosis. *American journal of respiratory and critical care medicine* 2018; **197**(9):
583 1198-208.
- 584 28. Sivakumaran D, Jenum S, Vaz M, et al. Combining host-derived biomarkers with patient
585 characteristics improves signature performance in predicting tuberculosis treatment outcomes.
586 *Communications Biology* 2020; **3**(1): 359.
- 587 29. Ugarte-Gil C, Alisjahbana B, Ronacher K, et al. Diabetes mellitus among pulmonary
588 tuberculosis patients from 4 tuberculosis-endemic countries: the TANDEM study. *Clinical Infectious*
589 *Diseases* 2020; **70**(5): 780-8.
- 590 30. Viswanathan V, Kumpatla S, Aravindalochanan V, et al. Prevalence of diabetes and pre-
591 diabetes and associated risk factors among tuberculosis patients in India. *PLoS One* 2012; **7**(7):
592 e41367.
- 593 31. Restrepo BI, Camerlin AJ, Rahbar MH, et al. Cross-sectional assessment reveals high
594 diabetes prevalence among newly-diagnosed tuberculosis cases. *Bulletin of the World Health*
595 *Organization* 2011; **89**: 352-9.
- 596 32. Eckold C, Kumar V, Weiner J, et al. Impact of Intermediate Hyperglycemia and Diabetes on
597 Immune Dysfunction in Tuberculosis. *Clinical Infectious Diseases* 2021; **72**(1): 69-78.
- 598 33. Prada-Medina CA, Fukutani KF, Kumar NP, et al. Systems immunology of diabetes-
599 tuberculosis comorbidity reveals signatures of disease complications. *Scientific reports* 2017; **7**(1): 1-
600 16.
- 601 34. Ruslami R, Koesoemadinata RC, Soetedjo NNM, et al. The effect of a structured clinical
602 algorithm on glycemic control in patients with combined tuberculosis and diabetes in Indonesia: A
603 randomized trial. *Diabetes Research and Clinical Practice* 2021; **173**: 108701.
- 604 35. Dobin A, Davis CA, Schlesinger F, et al. STAR: ultrafast universal RNA-seq aligner.
605 *Bioinformatics* 2013; **29**(1): 15-21.
- 606 36. Andrews S. FastQC: a quality control tool for high throughput sequence data. 2010.
607 <http://www.bioinformatics.babraham.ac.uk/projects/fastqc2020>).
- 608 37. Anders S, Pyl PT, Huber W. HTSeq—a Python framework to work with high-throughput
609 sequencing data. *bioinformatics* 2015; **31**(2): 166-9.
- 610 38. Love MI, Huber W, Anders S. Moderated estimation of fold change and dispersion for RNA-
611 seq data with DESeq2. *Genome biology* 2014; **15**(12): 1-21.
- 612 39. Joosten S, Goeman J, Sutherland J, et al. Identification of biomarkers for tuberculosis disease
613 using a novel dual-color RT-MLPA assay. *Genes & Immunity* 2012; **13**(1): 71-82.
- 614 40. Benjamini Y, Hochberg Y. Controlling the false discovery rate: a practical and powerful
615 approach to multiple testing. *Journal of the Royal statistical society: series B (Methodological)* 1995;
616 **57**(1): 289-300.
- 617 41. Lever M RP, Nakaya H. mdp: Molecular Degree of Perturbation calculates scores for
618 transcriptome data samples based on their perturbation from controls. R package version 1.12.0. 2021.
619 <https://mdp.sysbio.tools/>.

- 620 42. Chikina M, Zaslavsky E, Sealfon SC. CellCODE: a robust latent variable approach to
621 differential expression analysis for heterogeneous cell populations. *Bioinformatics* 2015; **31**(10):
622 1584-91.
- 623 43. Abbas AR, Wolslegel K, Seshasayee D, Modrusan Z, Clark HF. Deconvolution of blood
624 microarray data identifies cellular activation patterns in systemic lupus erythematosus. *PLoS one* 2009;
625 **4**(7): e6098.
- 626 44. Novershtern N, Subramanian A, Lawton LN, et al. Densely interconnected transcriptional
627 circuits control cell states in human hematopoiesis. *Cell* 2011; **144**(2): 296-309.
- 628 45. Weiner 3rd J, Domaszewska T. tmod: an R package for general and multivariate enrichment
629 analysis. *PeerJ Preprints* 2016; **4**: e2420v1.
- 630 46. Nueda MJ, Tarazona S, Conesa A. Next maSigPro: updating maSigPro bioconductor package
631 for RNA-seq time series. *Bioinformatics* 2014; **30**(18): 2598-602.
- 632 47. Bates D, Mächler M, Bolker B, Walker S. Fitting linear mixed-effects models using lme4.
633 *arXiv preprint arXiv:14065823* 2014.
- 634 48. Gregorutti B, Michel B, Saint-Pierre P. Correlation and variable importance in random
635 forests. *Statistics and Computing* 2017; **27**(3): 659-78.
- 636 49. Chawla NV, Bowyer KW, Hall LO, Kegelmeyer WP. SMOTE: synthetic minority over-
637 sampling technique. *Journal of artificial intelligence research* 2002; **16**: 321-57.
- 638 50. Liaw A, Wiener M. Classification and regression by randomForest. *R news* 2002; **2**(3): 18-22.
- 639 51. Kuhn M. Building predictive models in R using the caret package. *Journal of statistical*
640 *software* 2008; **28**(1): 1-26.
- 641 52. Raudvere U, Kolberg L, Kuzmin I, et al. g:Profiler: a web server for functional enrichment
642 analysis and conversions of gene lists (2019 update). *Nucleic Acids Research* 2019; **47**(W1): W191-
643 W8.
- 644 53. Huang DW, Sherman BT, Lempicki RA. Bioinformatics enrichment tools: paths toward the
645 comprehensive functional analysis of large gene lists. *Nucleic acids research* 2009; **37**(1): 1-13.
- 646 54. Gebremicael G, Kassa D, Quinten E, et al. Host gene expression kinetics during treatment of
647 tuberculosis in HIV-coinfected individuals is independent of highly active antiretroviral therapy. *The*
648 *Journal of infectious diseases* 2018; **218**(11): 1833-46.
- 649 55. Gebremicael G, Kassa D, Alemayehu Y, et al. Gene expression profiles classifying clinical
650 stages of tuberculosis and monitoring treatment responses in Ethiopian HIV-negative and HIV-
651 positive cohorts. *PLoS One* 2019; **14**(12): e0226137.
- 652 56. Heyckendorf J, Marwitz S, Reimann M, et al. Prediction of anti-tuberculosis treatment
653 duration based on a 22-gene transcriptomic model. *European respiratory journal* 2021.
- 654 57. Moreira-Teixeira L, Mayer-Barber K, Sher A, O'Garra AJJoEM. Type I interferons in
655 tuberculosis: Foe and occasionally friend. *J Journal of Experimental Medicine* 2018; **215**(5): 1273-85.
- 656 58. del Rosario RCH, Poschmann J, Kumar P, et al. Histone acetylome-wide association study of
657 tuberculosis. *bioRxiv* 2019: 644112.
- 658 59. Sivakumaran D, Blatner G, Bakken R, et al. A 2-Dose AERAS-402 Regimen Boosts CD8+
659 Polyfunctionality in HIV-Negative, BCG-Vaccinated Recipients. *Frontiers in Immunology* 2021; **12**:
660 2141.
- 661 60. Sivakumaran D, Ritz C, GjØen JE, et al. Host blood RNA transcript and protein signatures for
662 sputum-independent diagnostics of tuberculosis in adults. *Frontiers in immunology* 2020; **11**: 3795.

663

664 **Tables**

665 **Table 1. Study Participant Demographics**

Characteristic	Country	TB Patients		Healthy Controls	P-value
		Good Outcome	Poor Outcome		
Total Number of Participants	S Africa	76	18	27	-
	Indonesia	61	21	0	-
	All	137	39	27	-
Age in years, median (range)	S Africa	46 (22-68)	42 (19-55)	42 (30-70)	0.485
	Indonesia	49 (25-73)	49 (35-68)	-	0.96
	All	47 (22-73)	47 (19-68)	42 (30-70)	0.2801
Sex, % male (No. male/ female)	S Africa	58 (44/32)	67 (12/6)	52 (14/13)	0.6981
	Indonesia	53 (32/29)	67(14/7)	-	0.3136
	All	56 (76/61)	67 (26/13)	52 (14/13)	0.2704
Number with Diabetes / Intermediate Hyperglycaemia / Normal glycaemia (%)	S Africa	13/49/14	4/11/3	0/0/27	0.8775 ^s
	Indonesia	31/16/14	11/3/6	-	0.5589
	All	44/65/28	15/14/9	0/0/27	0.5409^s
HbA1c median (range)	S Africa	6.0 (4.9-14.3)	6.0 (4.8-14.1)	5.3 (4.8-6.4)	0.6144 ^s
	Indonesia	8.15 (4.9-17.1)	7.1 (5.1-14.1)	-	0.5612
	All	6.0 (4.9-17.1)	6.1 (4.8-14.1)	5.3 (4.8-6.4)	0.9892^s
BMI at TB diagnosis:, median (range)	S Africa	18.7 (13.9-32.3)	18.3 (13.7-31.2)	23.7 (17.4-45.2)	0.9588 ^s
	Indonesia	19.7 (13.8-33.3)	18.8 (16.3-27.3)	-	0.8433
	All	19.1 (13.8-33.3)	18.8 (13.7-31.2)	23.7 (17.4-45.2)	0.8351^s
TTP (days) at TB diagnosis: Median (range) (missing values)	S Africa	6 (1-21) (18)	6 (3-21) (3)	N/A	0.8916
Smear Grade at diagnosis number: 3+/2+/1+/scanty/negative	Indonesia	16/23/14/2/6	8/4/6/2/1	N/A	0.3637
Sputum conversion at Month 2: number yes/no (missing values)	S Africa	49/19 (8)	10/6 (2)	N/A	0.4518
	Indonesia	44/15 (2)	10/8 (2)	N/A	0.1227
	All	93/34 (10)	20/14 (4)	N/A	0.1029
Outcome classification: Cured /Recurrence/Failed/Died	S Africa	76/0/0/0	0/4/10/4	N/A	<0.0001
	Indonesia	61/0/0/0	0/2/16/3	N/A	<0.0001
	All	137/0/0/0	0/6/26/7	N/A	<0.0001
RNASeq subset	S Africa	26	6	0	-
	Indonesia	23	8	0	-
	All	49	14	0	-
MLPA subset	S Africa	76	18	27	-
	Indonesia	58	21	0	-
	All	135	39	27	-

666 \$ Comparison of TB patients with Good or Poor TB treatment outcome, HC excluded

667 **Table 2. Clusters of genes differentially expressed between TB patients with good or poor treatment**
 668 **outcomes to TB treatment in MaSigPro analysis of combined RNA-Seq data from South Africa and**
 669 **Indonesia**

Cluster Number	Overall pattern	Number of gene transcripts	Gene Function				Top Functions from g:Profiler** with adjusted P<0.05
			Protein Coding	Processed Transcript	Pseudo-gene	Regulatory RNAs*	
1	↓ through treatment; Higher in Good at W2	26	20	1	0	5	GO:MF – Opsonin Binding; GO:CC – Intracellular Vesicles; Endomembrane System
2	↑ through treatment; Higher in Poor throughout	14	13	0	0	1	GO:BP – B cell receptor (BCR) signaling; GO:CC – BCR complex KEGG – BCR signaling; primary immunodeficiency; REAC – BCR signaling WP – BCR signaling CORUM – CIN85-BLNK complex
3	↑ through treatment; Higher in Good at W26	25	17	2	0	6	<i>No significant results</i>
4	↓ through treatment; Higher in Poor throughout	47	37	2	2	6	GO:CC – Arp2/3 complex; KEGG – Shigellosis; E.coli, Yersinia, Salmonella infection; Endocytosis; REAC – Ephrin signaling; Rho GTPases activate WASPs and WAVES; TF – ZNF544 CORUM – Arp2/3 complex
5	Small ↓ through treatment; Higher in Poor throughout	11	6	1	1	3	GO:MF – L-tyrosine transmembrane transporter activity; GO:BP – positive regulation of fatty acid transport.
6	No change; Higher in Poor throughout	4	0	0	3	1	<i>No significant results</i>
7	↑ to W2, then ↓; Higher in Poor at W2	4	4	0	0	0	GO:BP – mitotic cell cycle process WP – Retinoblastoma Gene in Cancer
8	↑ in Good through treatment; No change in Poor	7	3	0	2	2	GO:MF – RNA polymerase III activity
9	↓ through treatment; Much greater change in Good	10	10	0	0	0	GO:MF – immunoglobulin receptor binding GO:BP – phagocytosis, recognition; complement activation, classical pathway; immunoglobulin mediated immune response; B cell activation GO:CC – immunoglobulin complex; E/C space; plasma membrane REAC – Classical antibody-mediated complement activation; FCGR activation; phagocytosis.

670 *Retained introns, Antisense, LncRNA, miRNA, nonsense-mediated decay, sense overlapping, sense intronic,
 671 snoRNA,
 672 **Redundant G:Profiler results are not shown

673 **Table 3. dcRT-MLPA Gene signatures Good versus Poor obtained by pooling the study groups and the**
 674 **cohorts**
 675

Diagnosis Signature

Gene	Module
GBP1	IFN signaling genes
FCGR1A	IFN signaling genes
STAT1	IFN signaling genes
IFITM3	IFN signaling genes
BCL2	Apoptosis - Survival
CCL4	Treg associated genes
TLR9	Pattern recognition receptors
CD274	IFN signaling genes

Week two Signature

Gene	Module
GBP5	IFN signaling genes
INDO	IFN signaling genes
GBP1	IFN signaling genes
BMP6	Cell growth - proliferation
CXCL9	Chemokines
GATA3	Th2 associated genes
FCGR1A	IFN signaling genes
MMP9	Inflammation
PTPRCv1	T cell subset markers
SPP1	Inflammation
CD3E	T cell subset markers
ASAP1	Small GTPases - (Rho) GTPase activating proteins
IL5	Th2 associated genes
TNFRSF1B	Apoptosis - Survival
NLRP2	Inflammasome components
MRC1	Pattern recognition receptors
NLRP6	Inflammasome components
IL22RA1	Th17 associated genes
VEGF	Cell growth - proliferation
KIF1B	Intracellular transport
CCL19	Chemokines
CD209	Pattern recognition receptors

Month 2 Signature

Gene	Module
BLR1	G protein-coupled receptors
BMP6	Cell growth - proliferation
CCL13	Chemokines
GBP1	IFN signaling genes
GBP2	IFN signaling genes
GBP5	IFN signaling genes
IFI16	IFN signaling genes
IL9	Th9 associated genes
INDO	IFN signaling genes
MMP9	Inflammation
NOD2	Pattern recognition receptors
OAS3	IFN signaling genes
PTPRCv2	T cell subset markers
TAP1	IFN signaling genes

Genes that appeared in more than one gene signature (diagnosis, week two or month two) are shown in bold. Gene signatures were obtained by down-sampling the majority class (good treatment outcome).

676

677 **Figure legends**

678 **Figure 1. MDP plots representing the change in gene expression perturbation in TB patients categorized**
679 **based on treatment outcome.** Full blood transcriptomes from TB patients who had a good or poor treatment
680 outcome were determined by (A) RNA-Seq and by (B) dcRT-MLPA. The extent of overall difference in gene
681 expression, relative to the median of expression at diagnosis in those who had a good treatment outcome, was
682 calculated for individual patients at the timepoints shown. The bars and whiskers show the median and data within
683 the $Q_1-1.5 \times$ inter quartile range (IQR) and $Q_3+1.5 \times$ IQR interval. Differences were significant by Mann-Whitney
684 U-test with Benjamini-Hochberg correction for multiple testing. * $p<0.05$, ** $p<0.01$, *** $p<0.001$, ****
685 $p<0.0001$.

686
687 **Figure 2. MaSigPro analysis of TB patients with good or poor treatment outcome, across combined South**
688 **African and Indonesian cohorts.** Plots show hierarchical clusters of genes in patients with a good (blue) or poor
689 (red) treatment outcome. Bars show mean \pm 1 SEM. Data were filtered to remove lowly abundant transcripts prior
690 to analysis.

691
692 **Figure 3. DEA of all TB patients from the pooled (South African and Indonesian) cohorts categorized based**
693 **on treatment outcome compared to their gene expression levels at diagnosis.** (A) Volcano plots representing
694 DEGs regulated during anti-TB treatment of TB patients who had a good treatment outcome (left panel) or a poor
695 treatment outcome (right panel). The y-axis scales of the plots are harmonized per treatment outcome. $-\log_{10}$ -
696 transformed p-values are plotted against \log_2 FC. Genes with $p<0.05$ and \log_2 FC <-0.6 or >0.6 were labelled as
697 DEGs. (B) Heatmaps displaying \log_2 FC of the DEGs and corresponding gene modules. The saturation of color
698 represents the magnitude of differential expression. Differences were significant by means of linear mixed models.
699 * $p<0.05$, ** $p<0.01$, *** $p<0.001$, **** $p<0.0001$.

700
701 **Figure 4. Prediction of treatment outcome in dcRT-MLPA data from peripheral blood.** (A) ROC curves
702 showing the predictive power of the gene signatures identified in the balanced pooled cohort (South Africa and
703 Indonesia) to classify TB patients at diagnosis (left panel), two weeks (middle panel) or two months (right panel)
704 after initiation of anti-TB treatment into patients who had a good treatment outcome and patients who had a poor
705 treatment outcome, using the RFE-RF model and LOOCV. The dataset was balanced by down-sampling to
706 encompass the same number of individuals with poor and good treatment outcome (diagnosis, $n=34$; week two,
707 $n=33$; month two, $n=34$). (B) Gene expression kinetics of the single genes encompassing the diagnosis or week
708 two gene signatures predicting treatment outcome in the pooled cohort. Box plots depict *GAPDH*-normalized,
709 \log_2 -transformed median gene expression values and the IQR, while the whiskers represent the data within the
710 $Q_1-1.5 \times$ IQR and $Q_3+1.5 \times$ IQR interval. (C). ROC curves showing the predictive power of the gene signatures
711 identified in the balanced pooled cohort (South Africa and Indonesia) to classify TB patients from an external
712 validation cohort (India) at diagnosis (left panel) or two months (right panel) after initiation of anti-TB treatment
713 into patients who had a good treatment outcome and patients who had a poor treatment outcome. The dataset was
714 balanced by down-sampling to encompass the same number of individuals with poor and good treatment outcome
715 (diagnosis, $n=22$; month two, $n=22$). Abbreviations: AUC, area under the curve; CI, confidence interval.

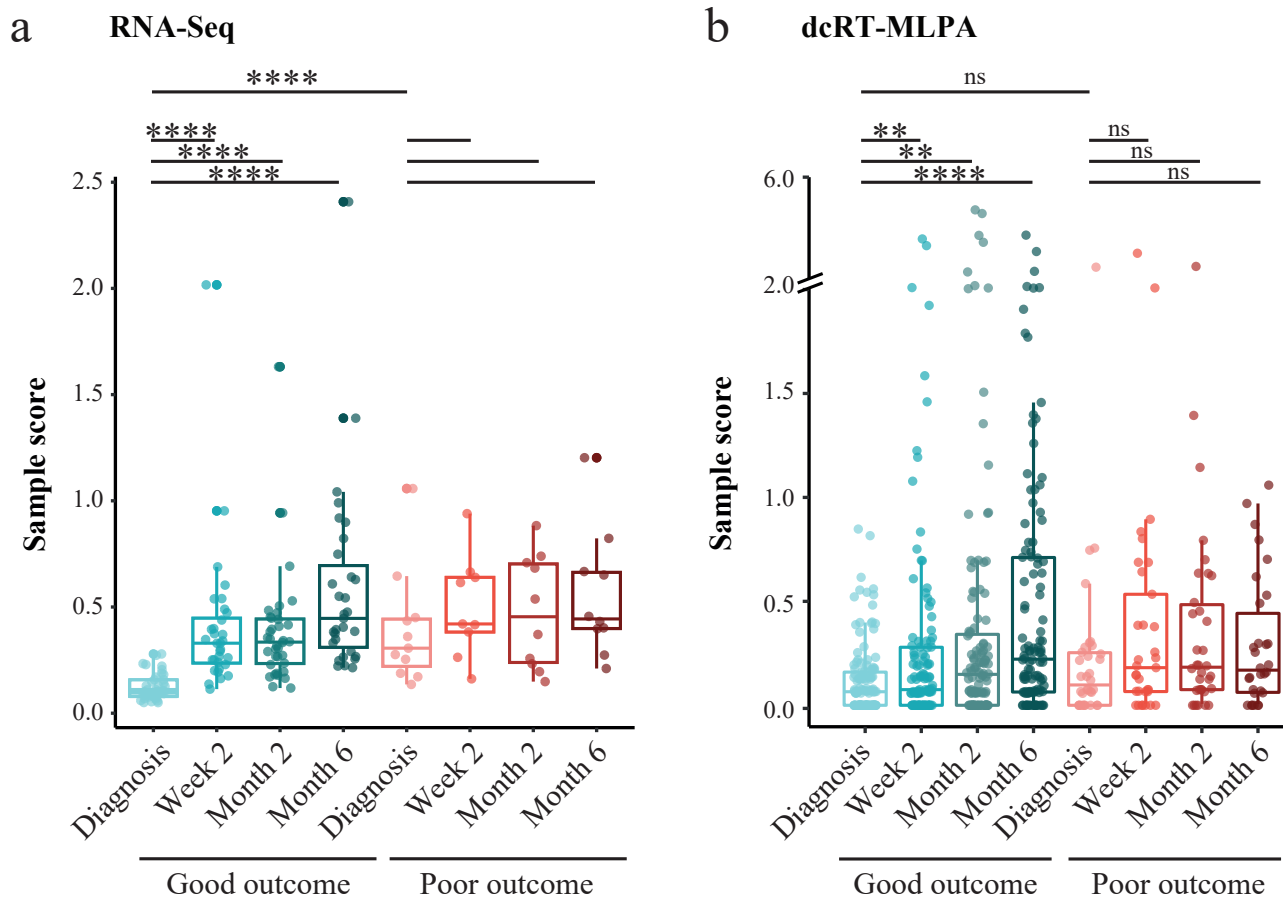


Figure 1

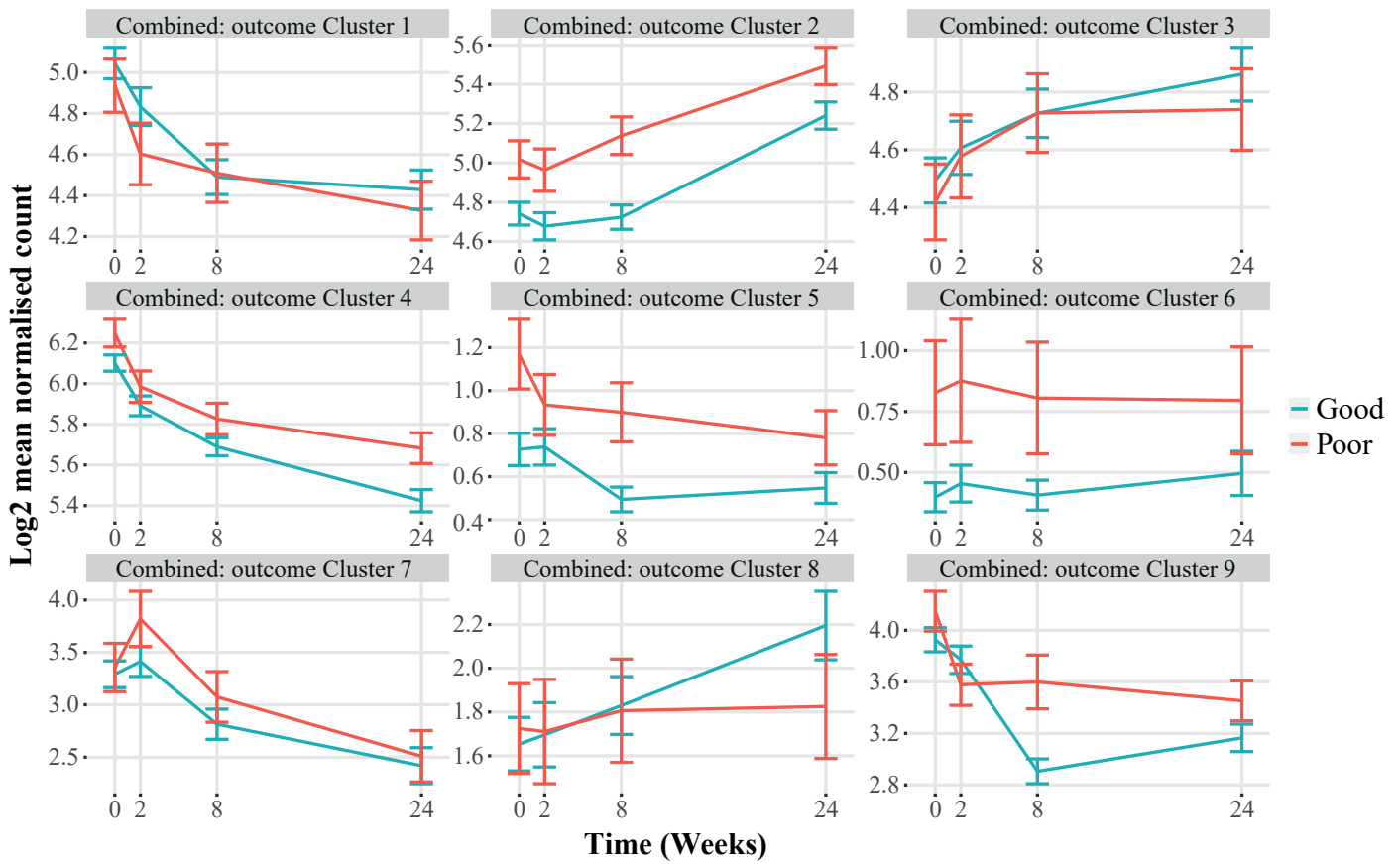


Figure 2

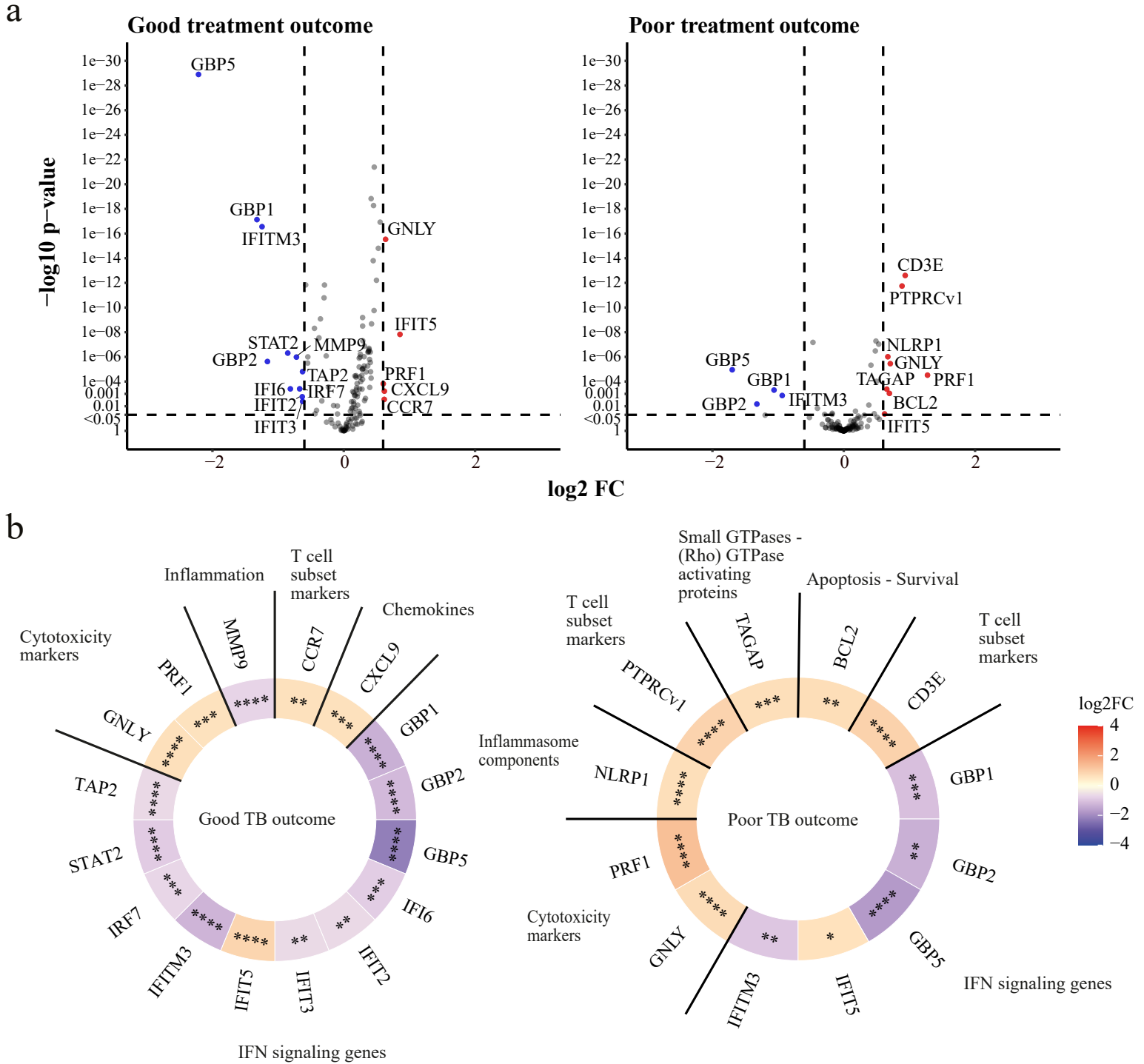


Figure 3

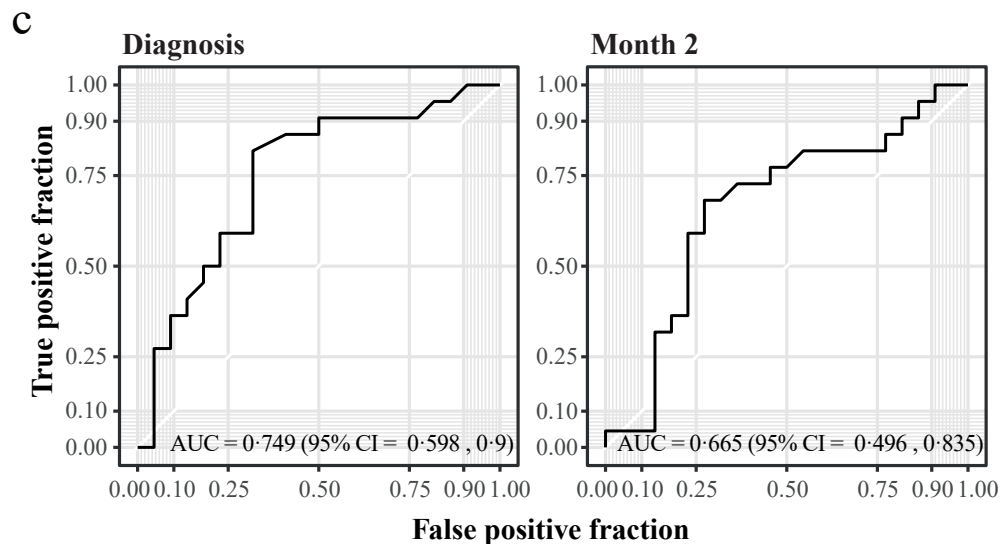
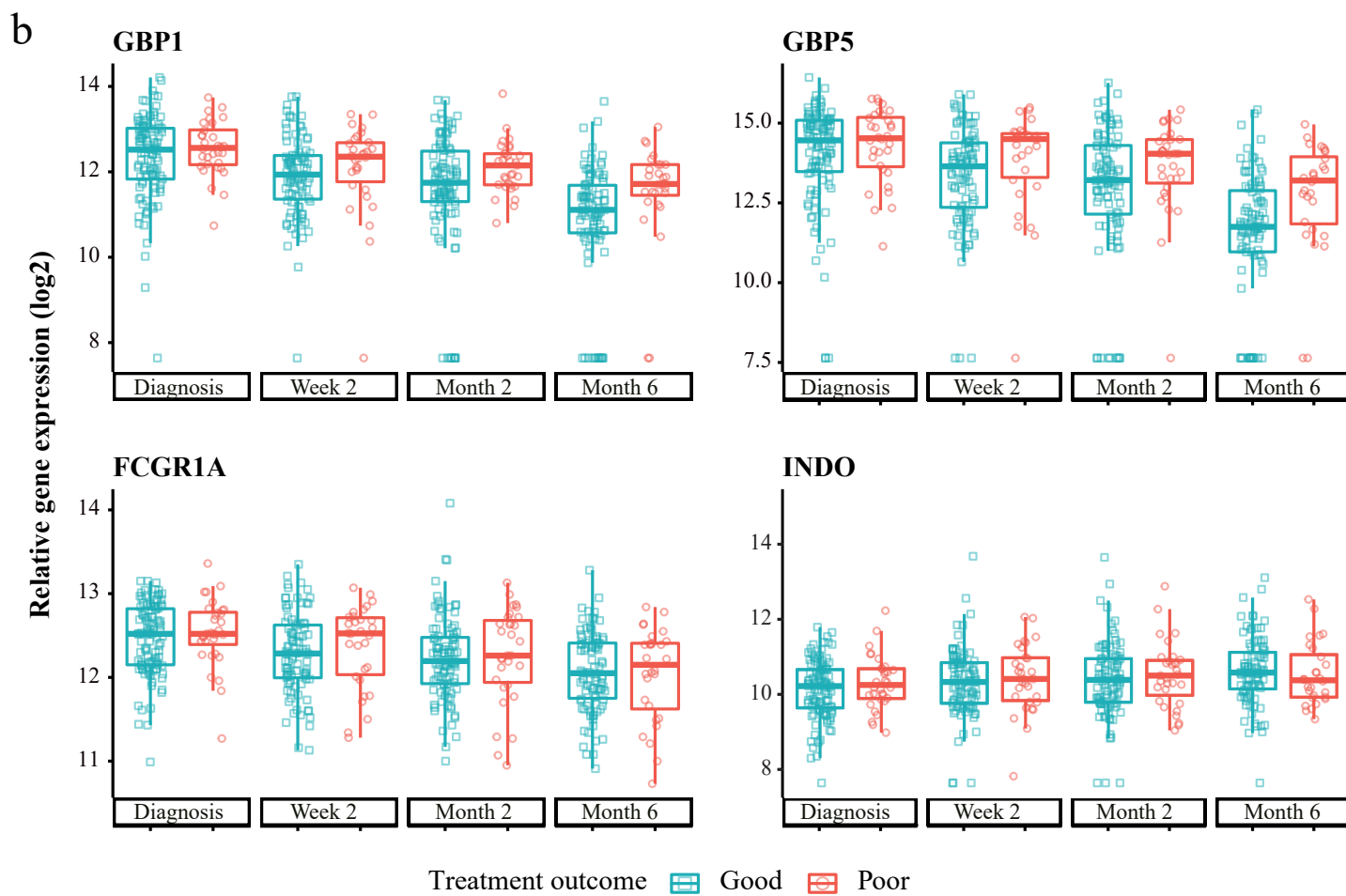
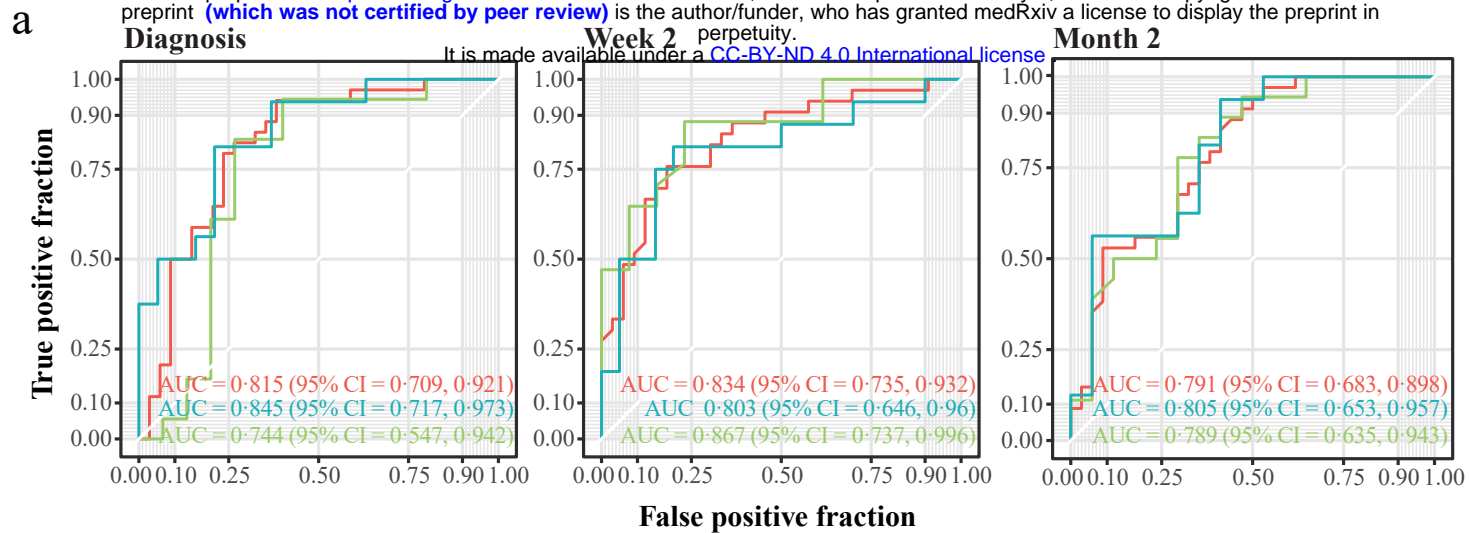


Figure 4

714 **Supplementary Information**

715 *Reverse-Transcriptase Multiplex Ligation-dependent Probe Amplification (dcRT-MLPA)*

716 For each target-specific sequence, a specific RT primer was designed located immediately
717 downstream of the left- and right-hand half-probe target sequence. 125 ng RNA was reverse
718 transcribed to cDNA by incubation at 37°C for 15 min, using RT-primer mix and Moloney
719 Murine Leukemia Virus (M-MLV) reverse transcriptase (Promega, Leiden, The Netherlands).
720 Reverse transcriptase was inactivated by heating at 98°C for two minutes. The left- and right-
721 hand half probes were hybridized to the cDNA at 60°C overnight and annealed half-probes
722 were ligated at 54°C for 15 minutes using ligase-65 (MRC-Holland). Ligase-65 was
723 subsequently inactivated by heating at 98°C for five minutes. Ligated probes were amplified
724 by PCR: 33 cycles at 95°C for 30 seconds, 58°C for 30 seconds and 72°C for 60 seconds,
725 followed by one cycle at 72°C for 20 minutes. PCR products were 1:10 diluted in Highly
726 deionized (Hi-Di) formamide (ThermoFisher) containing 400HD Rhodamine X (ROX)
727 fluorophore size standard (ThermoFisher). PCR products were denatured at 95°C for five
728 minutes, stored immediately at 4°C and analyzed on an Applied Biosystems 3730 capillary
729 sequencer in GeneScan mode (BaseClear, Leiden, The Netherlands). Trace data were analyzed
730 using GeneMapper software 5 (Applied Biosystems, Warrington, UK). The areas of each
731 assigned peak (arbitrary units) were exported for analysis in R (version 3.6.3). Data were
732 corrected for batch effect and normalized to housekeeping gene glyceraldehyde 3-phosphate
733 dehydrogenase (*GAPDH*). Signals below the threshold value for noise cutoff
734 in GeneMapper (log₂ transformed peak area 7.64) were assigned the threshold value for noise
735 cutoff.

736 RT primers and half-probes were designed by Leiden University Medical Centre
737 (LUMC, Leiden, The Netherlands) and comprised sequences for four housekeeping genes and

738 144 selected key immune-related genes to profile the following compartments of the human
739 immune response (Supplementary Table S1): (1) Adaptive immune responses: T-cell
740 responses; Th1 responses; Th2 responses; Th17/22 responses; Treg responses; T-cell
741 cytotoxicity; Immune cell subset markers including B-cells and NK-cells. (2) Innate immune
742 responses: Myeloid-associated markers and scavenger receptors; Pattern recognition receptors;
743 Inflammasome components. (3) Inflammatory and IFN-signalling genes. (4) Other genes: Anti-
744 microbial activity; Apoptosis/cell survival; E3 ubiquitin protein ligases; Small
745 GTPases/(Rho)GTPase activating proteins; Additional chemokines; Cell growth/proliferation;
746 Cell activation; Transcriptional regulators/activators; Intracellular transport; Mitochondrial
747 Stress/Proteasome; Inflammation.

748

749 Linear Mixed Models for identification of DEGs

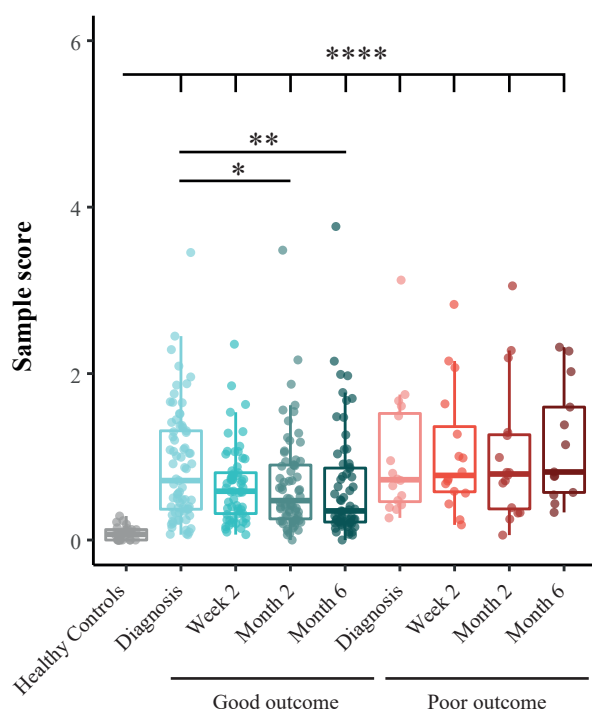
750 Longitudinal DEGs were identified by means of linear mixed models using the lmer function
751 of the lme4 package in R.⁴⁷ To increase statistical power, datasets of all TB patients included
752 in the South African and Indonesian cohorts were pooled independent of diabetes/glycaemia
753 status and split based on treatment outcome. Models were fitted on *GAPDH*-normalized log₂-
754 transformed targeted gene expression data. Outcome-time interactions were included as fixed
755 effects and the patients ID-time interactions were included as random effects.

756

757 Identification of gene signatures for treatment outcome

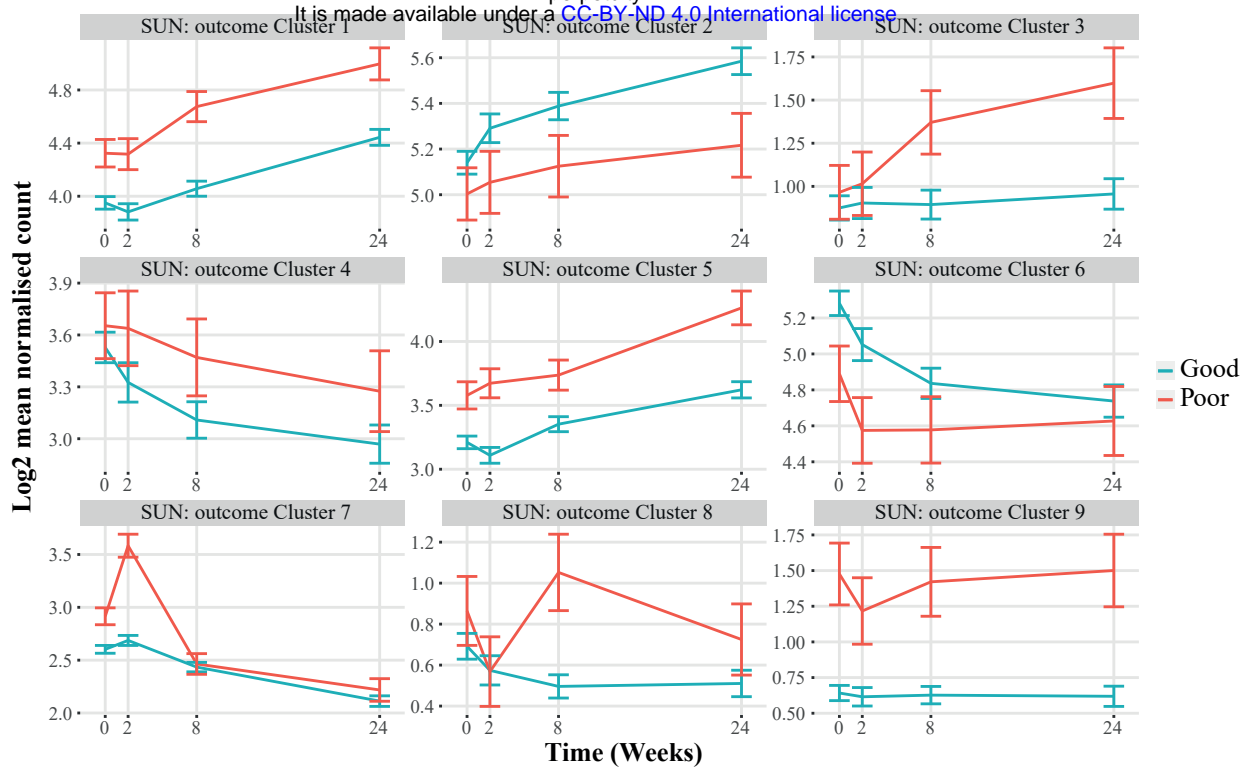
758 For modelling analyses, RNA-Seq data were randomly split into training and test sets (60/40)
759 using the R package *caret*.⁵¹ Feature selection was performed for each timepoint using RFE⁴⁸
760 with repeated cross validation as the re-sampling method (n=10). A weighted model was fitted
761 using glmnet method, using weights 1/frequency * 0.5 and repeated cross validation for re-
762 sampling (n=10). Each model was used to make predictions on the corresponding test set.

763 To identify signatures associated with treatment outcome in dcRT-MLPA data, TB
764 patients of South Africa and Indonesia were pooled independent of diabetes/glycaemia status.
765 To balance the dataset, we applied two random sampling approaches using R: (1) a down-
766 sampling approach, reducing the number of patients in the majority class (i.e. good treatment
767 outcome) and (2) an up-sampling approach by generating synthetic data from existing data
768 using the SMOTE⁴⁹ function from the *DMwR* package in R, resulting in equal numbers of
769 patients in both classes. Then, RFE⁴⁸, available in the *caret* R package⁵¹, was applied with K-
770 fold validation (K=10) to the entire data set search for the optimal combination and number of
771 top-ranking genes able to separate TB patients with a good and poor treatment outcome. RFE
772 is a powerful approach for variable selection in high-dimensional data by selecting features
773 that fit a model and removing the weakest feature (or features) until the specified number of
774 features is reached. Once the best predictors of treatment outcome were identified, the
775 expression values of these genes were extracted from the dataset. We subsequently applied
776 RF⁵⁰ as machine learning algorithm on the dataset and evaluated the performance by LOOCV,
777 both available on the *caret* R package.⁵¹

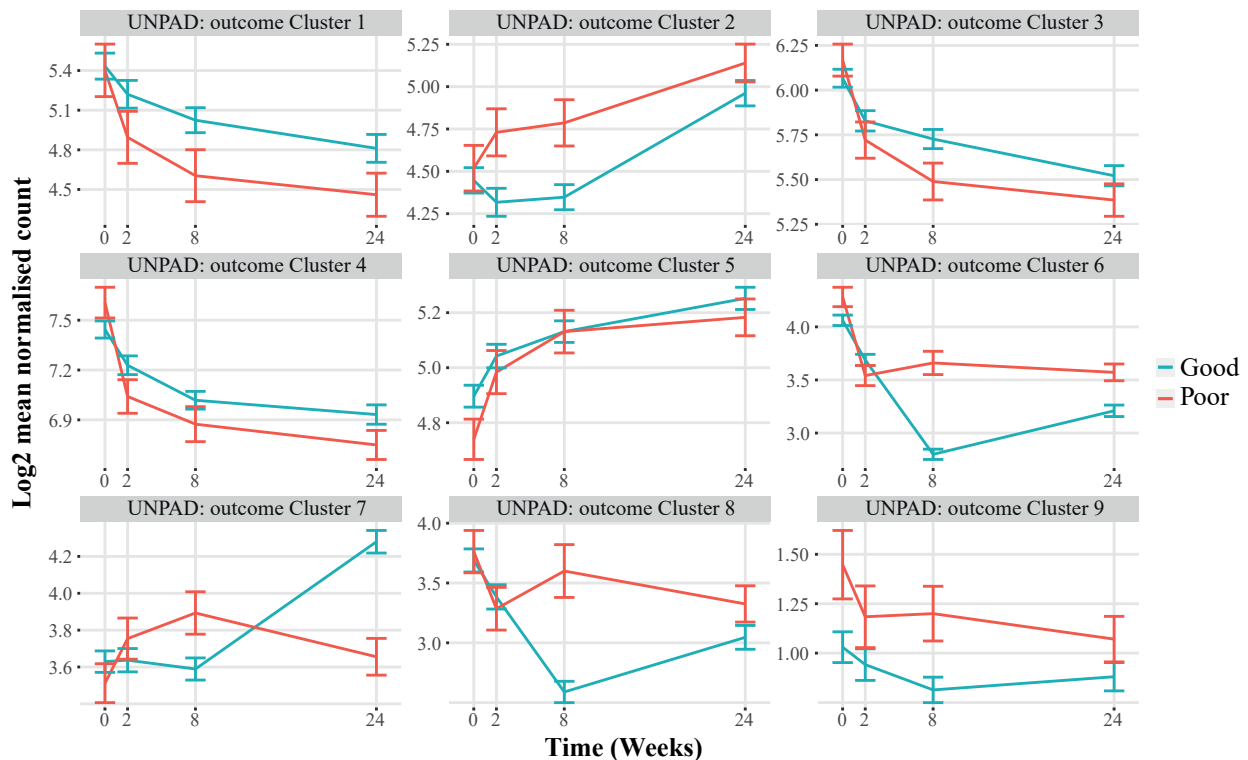


Supplementary Figure S1. MDP plot representing the change in gene expression perturbation in TB patients from South Africa categorized based on treatment outcome. Blood transcriptomes from TB patients who had a good or poor treatment outcome were determined by dcRT-MLPA. The extent of overall difference in gene expression, relative to the median of expression in healthy controls, was calculated for individual patients at the timepoints shown. The bars and whiskers show the median and data within the $Q1-1.5 \times \text{IQR}$ and $Q3+1.5 \times \text{IQR}$ interval. Differences were significant by Mann-Whitney U-test with Benjamini-Hochberg correction for multiple testing. * $p < 0.05$, ** $p < 0.01$, *** $p < 0.001$, **** $p < 0.0001$.

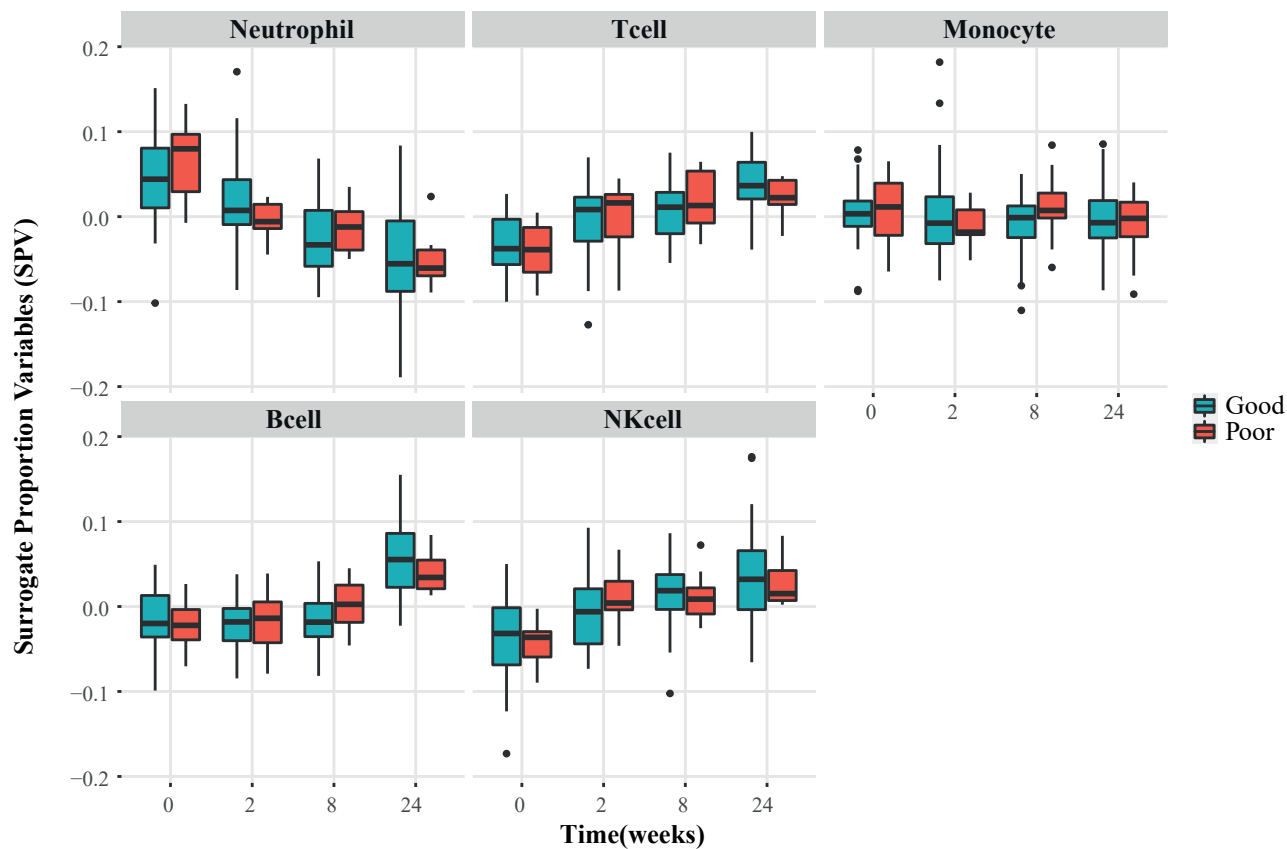
a



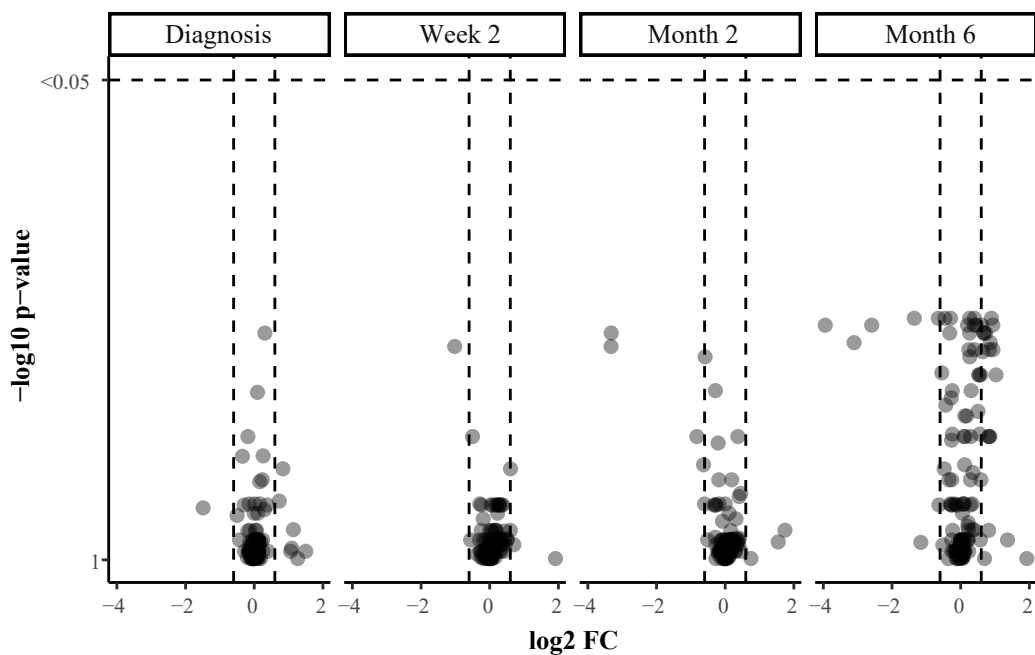
b



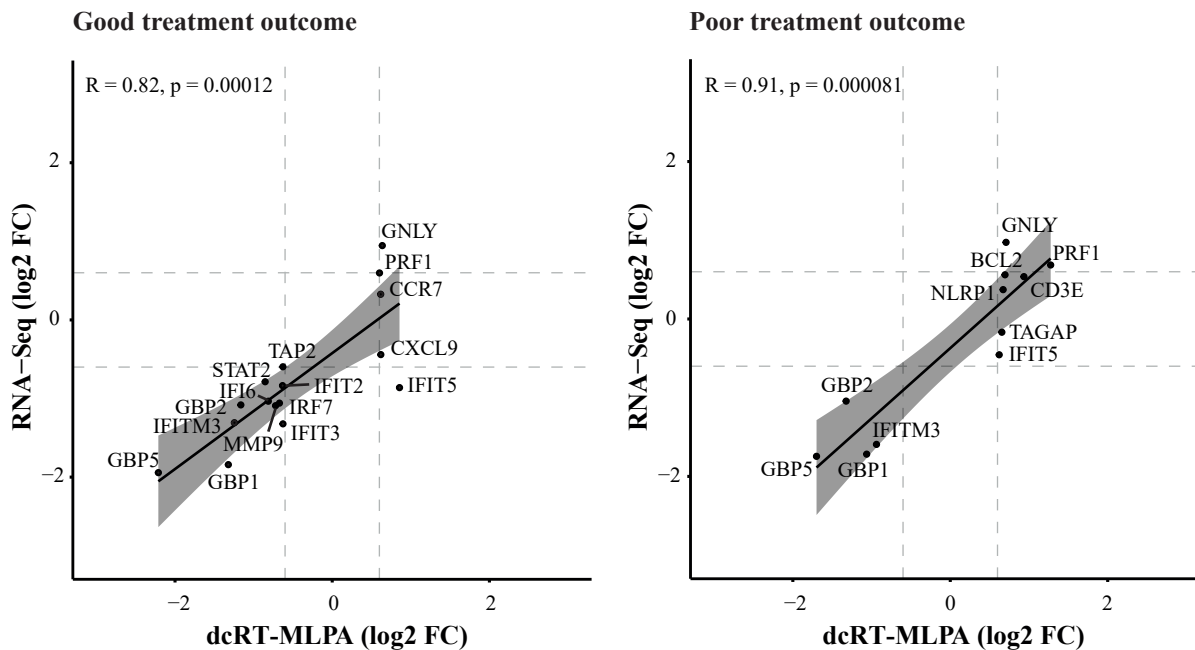
Supplementary Figure S2. Differential change in gene expression in TB patients through treatment in those who had a good or poor treatment outcome. MaSigPro analysis was conducted on the blood RNA-Seq data from TB patients from South Africa (a) or Indonesia (b), to identify genes which were significantly differentially expressed between those patients with a good or poor outcome. Plots show hierarchical clusters of genes, and bars show mean \pm 1 SEM. Data were filtered to remove lowly abundant transcripts prior to analysis.



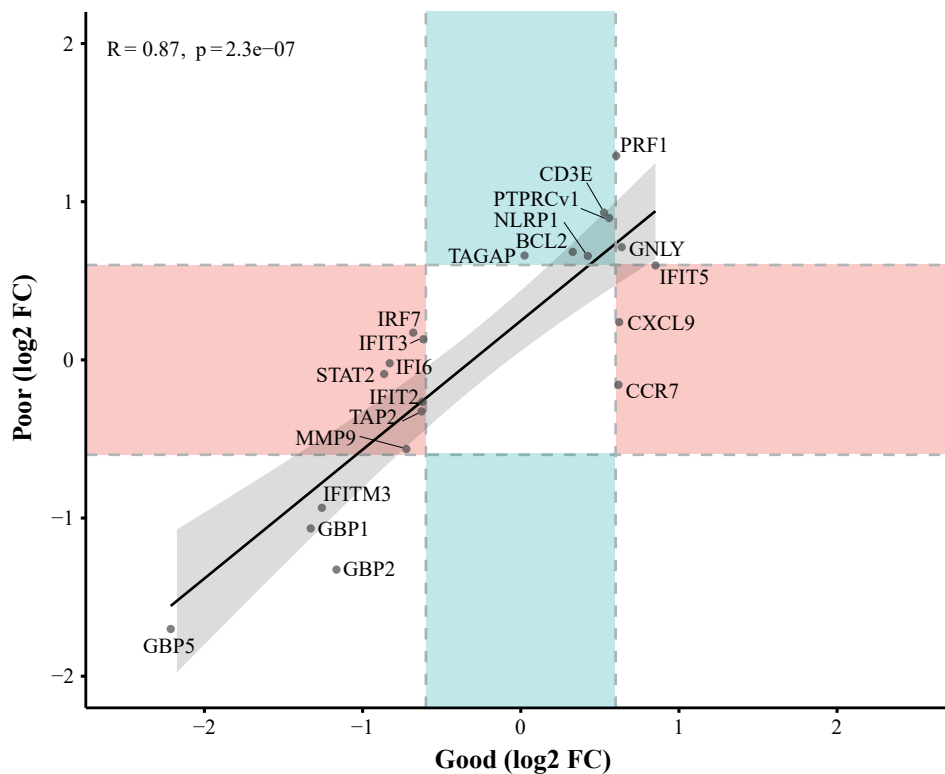
Supplementary Figure S3. Cell population estimates in good and poor treatment outcomes in South Africa and Indonesia. Estimates of relative differences in cell proportions were calculated from RNA-seq data using R package CellCODE. IRIS and DMAP data sets used as reference. Bars and whiskers show median and 1.5 x IQR.



Supplementary Figure S4. Differential expression analysis in patients from South Africa and Indonesia who had a poor treatment outcome versus patients who had a good treatment outcome at the indicated timepoints. Non-parametric Mann-Whitney U-test with Benjamini-Hochberg correction for multiple testing was applied to test for statistical differences between the groups.



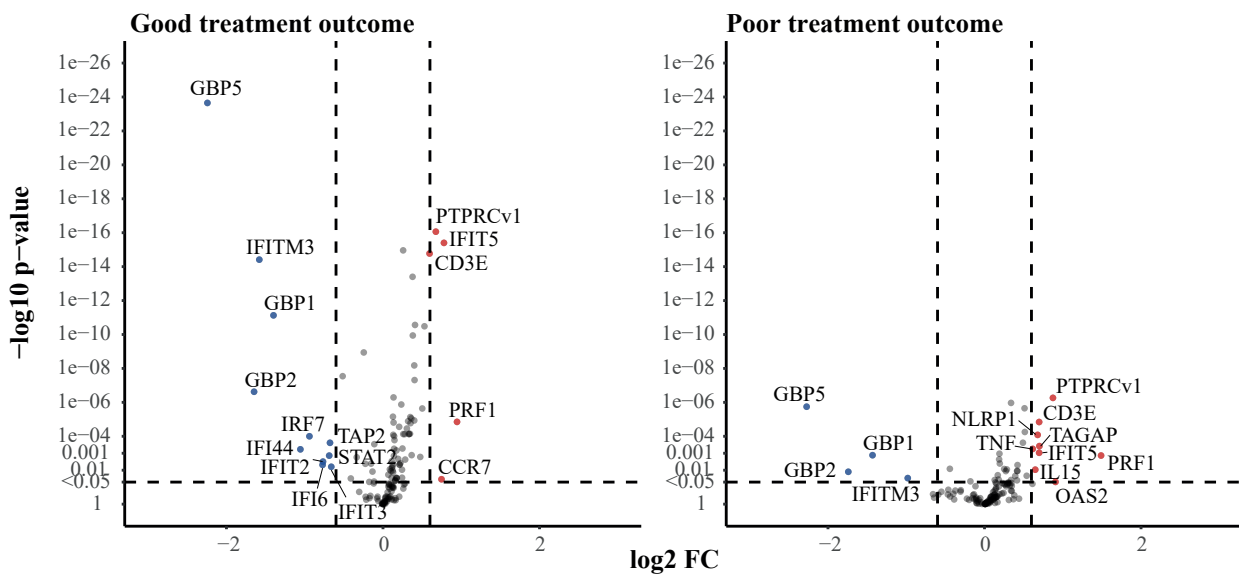
Supplementary Figure S5. Scatter plots representing Pearson correlations between the longitudinal DEGs identified by dcRT-MLPA versus the same genes identified by RNA-Seq. Values are plotted as log₂ FC (month six-diagnosis). Black line corresponds to line of best fit and shaded bands indicate confidence intervals.



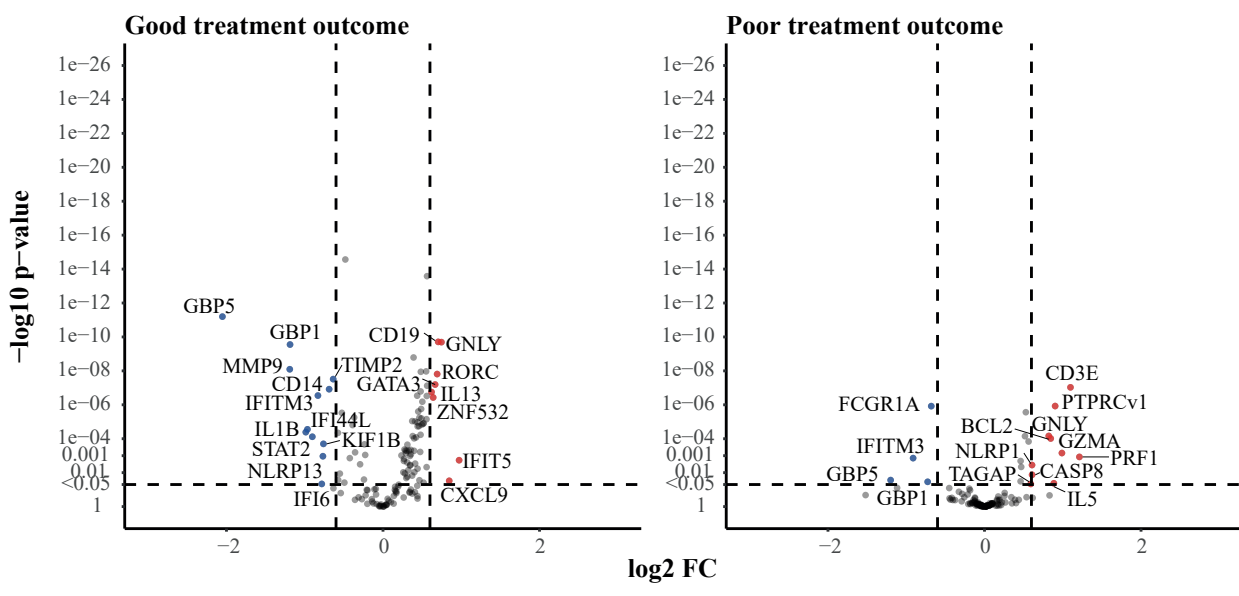
Supplementary Figure S6. Scatter plot representing Pearson correlations between the longitudinal DEGs in TB patients who had a poor treatment outcome versus the longitudinal DEGs in TB patients who had a good treatment outcome. Values are plotted as log₂ FC (month 6-diagnosis). Black line corresponds to line of best fit and shaded bands indicate confidence intervals. Red shaded areas indicate genes that were identified as DEGs only in patients who had a good treatment outcome and blue shaded areas indicate genes that were identified as DEGs only in patients who had a poor treatment outcome.

It is made available under a [CC-BY-ND 4.0 International license](https://creativecommons.org/licenses/by-nd/4.0/).

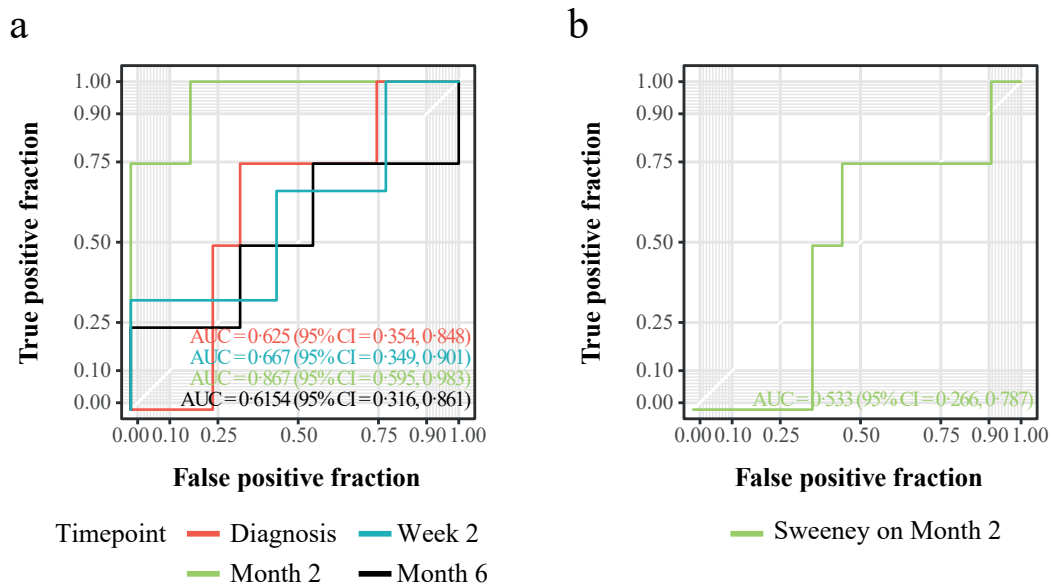
a



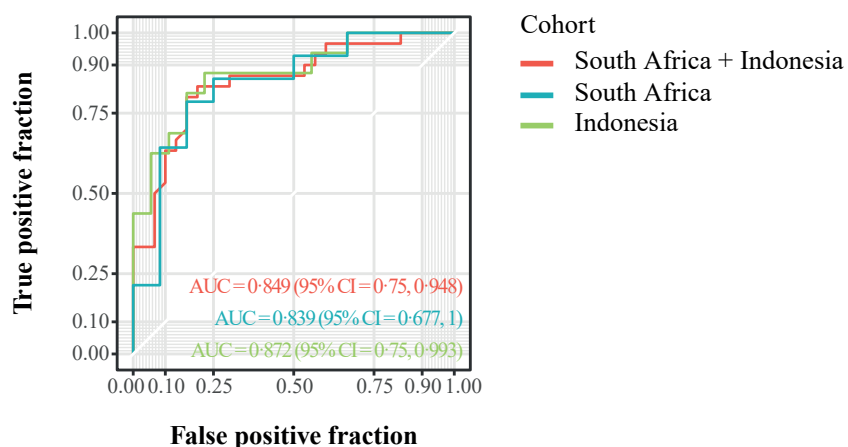
b



Supplementary Figure S7. Differential expression analysis of all TB patients from the South African and Indonesian cohorts categorized based on treatment outcome compared to their gene expression levels at diagnosis. (a) Volcano plots representing DEGs regulated during anti-TB treatment of TB patients from the South African cohort who had a good treatment outcome (left panel) or a poor treatment outcome (right panel). (b) Volcano plots representing DEGs regulated during anti-TB treatment of TB patients from the Indonesian cohort who had a good treatment outcome (left panel) or a poor treatment outcome (right panel). (a,b) The y-axis scales of the plots are harmonized per treatment outcome. $-\log_{10}$ -transformed p-values are plotted against $\log_2 FC$. Genes with $p < 0.05$ and $\log_2 FC < -0.6$ or > 0.6 were labelled as DEGs.

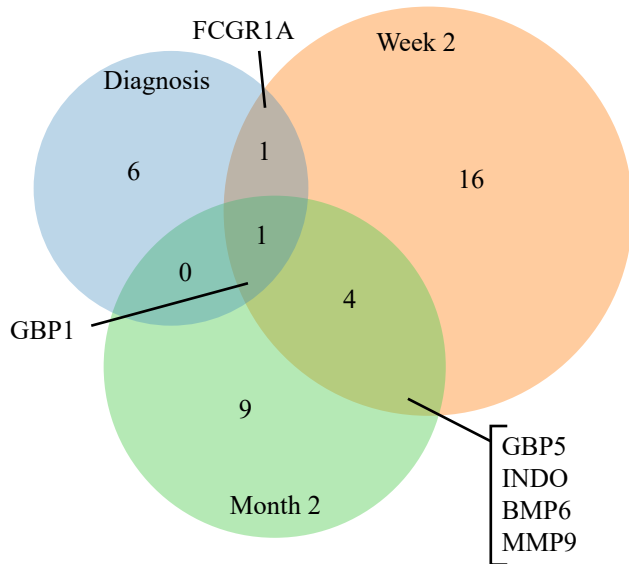


Supplementary Figure S8. Prediction of treatment outcome in RNA-Seq data from peripheral blood. ROC curves showing the predictive power of (a) the gene signatures identified in the pooled cohort (South Africa and Indonesia) or (b) the Sweeney gene signature to classify TB patients at the indicated timepoints after initiation of anti-TB treatment into patients who had a good treatment outcome and patients who had a poor treatment outcome. Data were split into training and test sets (60/40). For each time point a gene signature was generated by RFE and a weighted model fitted using glmnet method. Weights of $1/\text{frequency} * 0.5$ were used. Abbreviations: AUC, area under the curve; CI, confidence interval.

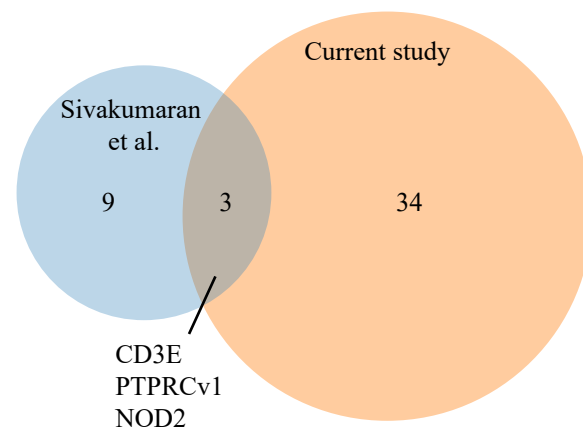


Supplementary Figure S9. Identification of a delta (week two minus diagnosis) signature predicting the outcome of anti-TB treatment. ROC curve showing the predictive power of the gene signature identified in the balanced pooled cohort to classify TB patients into patients who had a good treatment outcome and patients who had a poor treatment outcome, using the RFE - RF model and LOOCV. The dataset was balanced by down-sampling to encompass the same number of individuals with poor and good treatment outcome. Abbreviations: AUC, area under the curve; CI, confidence interval.

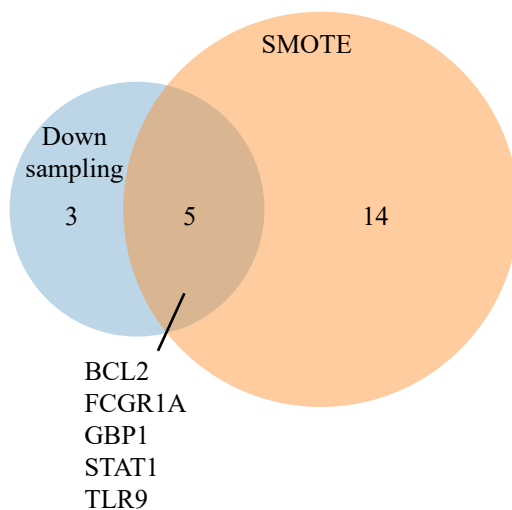
a Venn diagram - within cohort



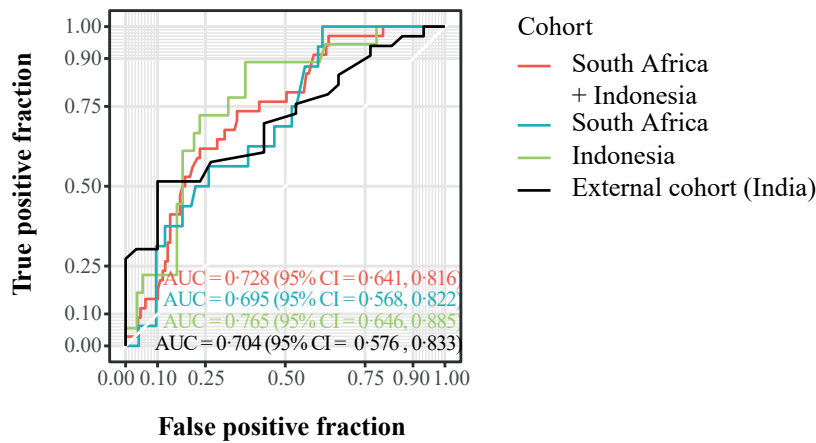
b Venn diagram - between cohorts



c Venn diagram - sampling methods at diagnosis



Supplementary Figure S10. Venn diagrams showing the number of genes encompassing treatment outcome signatures as identified by RFE-RF models. (a) Venn diagram displaying the number of unique and overlapping genes comparing diagnosis (blue), week two (orange) and month two (green) gene signatures obtained by random-downsampling. (b) Venn diagram displaying the number of unique and overlapping genes comparing the gene signatures in the current study (diagnosis, week two and month two; orange) obtained by random-downsampling with the gene signatures published by Sivakumaran et al. (blue). (c) Venn diagram displaying the number of unique and overlapping genes comparing the diagnosis gene signature obtained by random-downsampling (blue) with the diagnosis gene signature obtained by applying SMOTE sampling (orange) to balance the classes. Overlapping genes are annotated.



Supplementary Figure S11. Identification of a SMOTE diagnosis signature predicting the outcome of anti-TB treatment. ROC curves showing the predictive power of the gene signatures identified in the balanced pooled cohort (South Africa and Indonesia) and validated in the South African and Indonesian cohort or in an external Indian cohort. TB patients are classified into patients who had a good treatment outcome and patients who had a poor treatment outcome at diagnosis, using the RFE - RF model and LOOCV. The dataset was balanced by SMOTE to encompass the same number of individuals with poor and good treatment outcome. Abbreviations: AUC, area under the curve; CI, confidence interval.

Supplementary Table S1. List of target genes for dcRT-MLPA.

Module	Gene
Immune cell subset markers - B cells	CD19
NK cells	NCAM1
T cell subset markers	CD3E
	CD4
	CD8A
	CCR7
	PTPRCv1
	PTPRCv2
	AIRE
	IL7R
Th1 associated / IFN signaling genes	CXCL10
Th1 associated genes	IFNG
	IL1B
	IL2
	IL15
	TBX21
	TNF
Th2 associated genes	GATA3
	IL4
	IL482
	IL5
	IL6
	IL10
	IL13
Th9 associated genes	IL9
Th17 associated genes	IL17A
	RORC
	IL22RA1
Treg associated genes	CCL4
	CTLA4
	FOXP3
	IL2RA
	LAG3
	TGFB1
	TNFRSF18
Cytotoxicity markers	GZMA
	GZMB
	PRF1
Apoptosis / Survival	CASP8
	BCL2
	FASLG
	FLCN1
	TNFRSF1A
	TNFRSF1B
Myeloid-associated genes	CD14
	CD163
	CCL2
	CCL3

	CCL5 CCL22 CXCL13 IL12A IL12B IL23A FPR1
Chemokines	CCL11 CCL13 CCL19 CXCL9 CX3CL1
Pattern recognition receptors	CD209 CLEC7A MRC1 MRC2 NOD1 NOD2 TLR1 TLR2 TLR3 TLR4 TLR5 TLR6 TLR7 TLR8 TLR9 TLR10
Inflammasome components	NLRC4 NLRP1 NLRP2 NLRP3 NLRP4 NLRP6 NLRP7 NLRP10 NLRP11 NLRP12 NLRP13
IFN signaling genes	CD274 FCGR1A GBP1 GBP2 GBP5 IFI6 IFI16 IFI35

	IFI44 IFI44L IFIH1 IFIT2 IFIT3 IFIT5 IFITM1/3 INDO IRF7 OAS1 OAS2 OAS3 SOCS1 STAT1 STAT2 TAP1 TAP2
Inflammation	DSE MMP9 SPP1 TIMP2 TNIP1
Cell growth / Proliferation	BMP6 TGFBR2 AREG EGF VEGF
Cell activation	HCK LYN SLAMF7
Small GTPases / (Rho) GTPase activating proteins	ASAP1 RAB13 RAB24 RAB33A TAGAP TBC1D7
Anti-microbial activity	BPI LTF
E3 ubiquitin protein ligases	NEDD4L
Scavenger receptors	MARCO
G protein-coupled receptors	BLR1
Transcriptional regulators/activators	CAMTA1 TWIST1 ZNF331 ZNF532
Intracellular transport	SEC14L1 KIF1B
Mitochondrial Stress / Proteasome	HPRT
Housekeeping	ABR B2M GAPDH GUSB

Supplementary Table S7. Gene signatures for each timepoint - RNA-Seq

<u>Diagnosis</u>	<u>Week 2</u>	<u>Month 2</u>	<u>Month 6</u>
MADCAM1	FGFR3	CD79B	DNMT3B
MTFR2	ICAM3	PIK3CB	HAUS4
TM4SF1	SLC7A4	MEF2BNB-MEF2B	SLC22A18
CLCN1	PACSIN2	TCL1A	RTN4
WASF4P	HPN	TANGO6	CCRL2
ANKDD1B	ERGIC1	PTGES3	SERPINE2
HIST1H2BO	IL1R2	DOCK7	LYSM2
TCTEX1D2	SSPN	ZNHIT6	WASH2P
RPSAP54	DOK4	KIF14	IL17RC
WASH4P	PRKCG	PARD6B	ARFIP1
AC026185.1	TCN1	E2F5	CCDC68
RPS2P44	GCM1	AK7	PPP1R14A
RP11-466P24.6	GAS2L3	MPZL2	RIMBP3
RP11-1105G2.4	SYT2	AKR1E2	Y_RNA
RP11-229P13.25	NR1I2	OXSR1	MIR140
MIR3136	TENM4	CNIH2	LEPROT
CTB-50L17.9	SLC45A3	ACBD7	RPL18P10
RP11-272L13.4	WNK2	TNF	AC099552.2
RP11-92K15.3	DPCD	PTGES3L	RP11-544A12.5
RP11-305L7.7	CXCL11	SPIB	FLT1P1
	B3GALNT1	USP32P1	RP11-295K2.3
	SLC22A1	IGHD	RP11-56M3.1
	HIST1H2AJ	GOLGA2P7	AC132186.1
	SNRNP35	AC096579.7	C1orf213
	CLCN1	RP11-458F8.1	UGDH-AS1
	CTD-3088G3.8	AC002543.2	RP11-175P13.3
	SULF2	IGKV1D-16	RP11-638I2.10
	CLEC4C	LINC00617	RP11-705O1.8
	RNU6-1079P	RP11-407G23.4	SEN3-EIF4A1
	AGAP7	RP11-588K22.2	RP11-401F2.3
	STARD7-AS1	RP11-325K4.2	RP11-1109F11.3
	YBX1P1	AL133153.1	U91328.22
	PRRT4	RP11-479F13.1	
	LINC01001		
	BCAS2P2		
	RP11-459O1.2		
	AL627309.1		
	IFNG-AS1		
	CTD-3051D23.4		
	RP4-647C14.3		
	CTD-2006K23.1		
	RP11-457M11.5		
	BX649553.4		
	CTB-39G8.3		
	MUC8		
	AC092299.8		

Supplementary Table S8. Delta signature Good vs Poor obtained by pooling the study groups and the cohorts.

Delta (Week two - Diagnosis) Signature

Gene	Module
GPLY	Cytotoxicity markers
MRC1	Pattern recognition receptors
GBP5	IFN signaling genes
NLRP1	Inflammasome components
FLCN1	Apoptosis - Survival
ZNF532	Transcriptional regulators - activators
IFIT2	IFN signaling genes

Genes that appeared also in the diagnosis or week two gene signatures are shown in bold. Gene signatures were obtained by downsampling the majority class (Good treatment outcome).

Supplementary Table S9. SMOTE signature Good vs Poor obtained by pooling the study groups and the cohorts.

Diagnosis Signature

Gene	Module
AREG	Cell growth - proliferation
BCL2	Apoptosis - Survival
CASP8	Apoptosis - Survival
CCL13	Chemokines
CD209	Pattern recognition receptors
CLEC7A	Pattern recognition receptors
CTLA4	Treg associated genes
CX3CL1	Chemokines
FCGR1A	IFN signaling genes
GBP1	IFN signaling genes
IL12B	Myeloid associated genes
LTF	Anti-microbial activity
NLRP3	Inflammasome components
STAT1	IFN signaling genes
TIMP2	Inflammation
TLR8	Pattern recognition receptors
TLR9	Pattern recognition receptors
TNFRSF1A	Apoptosis - Survival
ZNF331	Transcriptional regulators - activators

Gene signature obtained by applying SMOTE sampling technique. Genes that are also identified in the Diagnosis signature obtained by downsampling are shown in bold.